



NTNU – Trondheim
Norwegian University of
Science and Technology

Rotor Design of Permanent Magnet Synchronous Machine for Pumped-storage Plant

Svein Christian Wedum

Master of Energy and Environmental Engineering

Submission date: July 2015

Supervisor: Arne Nysveen, ELKRAFT

Co-supervisor: Ivar Vikan, Voith Hydro

Norwegian University of Science and Technology
Department of Electric Power Engineering

NORGES TEKNISK-NATURVITENSKAPELIGE UNIVERSITET

NTNU



MASTER THESIS

Kandidatens navn : Svein Christian Wedum

Fag : **ELKRAFTTEKNIKK**

Oppgavens tittel (norsk) : Rotordesign av PM synkrongenerator for pumpekraftverk

Oppgavens tittel (engelsk) : Rotor design of PM synchronous machine for pumped-storage plant

Description:

Pumped storage can be used as balancing power in order to integrate large-scale wind-power and small-scale hydropower.

This work focuses on using PM synchronous machines instead of traditional synchronous machines with field winding in combination with a power electronic converter. Typical power range is foreseen to be 5-20 MW.

A complementary literature survey, of what was presented in the specialization project may be required.

The project is mostly theoretical including design methods and development of dimensioning framework.

More specifically the work shall focus on:

- Evaluate and select a rotor design suitable for this purpose
- Develop analytical procedures (equations) for dimensioning the PM rotor.
- Redesign a synchronous machine with field winding using PM magnetisation.

Further details of the work are to be discussed with the supervisors during the project period.

Oppgaven gitt : 15. januar 2015
Oppgaven revidert: : 04. juni 2015
Besvarelsen leveres innen : 16. juli 2015
Besvarelsen levert :
Utført ved (institusjon, bedrift) : Inst. for elkraftteknikk/NTNU
Kandidatens veileder : Ivar Vikan, Voith Hydro
Faglærer : Professor Arne Nysveen

Trondheim, 4. juni 2015

Arne Nysveen
faglærer

Preface

This master thesis is carried out at the Department of Electric Power Engineering at Norwegian University of Science and Technology (NTNU) during the spring 2015.

I would like to thank my supervisor Professor Arne Nysveen at the Department of Electric Power Engineering, NTNU, for his valuable guidance and support during this study.

Additionally, I would thank PhD candidate Mostafa Valavi for his support and interest in my work.

Finally, I would like to express my gratitude to my friends and family, for their motivation and support, as well as assistance with the text editing in this thesis.

Svein Christian Wedum
Trondheim, July 2015

Abstract

This master thesis is partly a deeper study of which was presented in the specialization project, fall of 2014. The main objective have been to develop and design a permanent magnet synchronous machine for hydro power plant application. In this study, an analytical design tool for this purpose was developed through a Matlab script. The analytical calculations have been verified by use of finite element method analysis in machine no-load operation, and the design tool is found sufficiently accurate for this study.

As background, a literature survey was performed, which resulted in the base for developing the analytical design tool. The relevant equations are presented in the theoretical part of this thesis.

A synchronous machine at 18 MVA with field windings have been redesigned by use of permanent magnet magnetization. The stator bore diameter was kept constant at 3.51 m in all machines simulated. At a decreased air gap of 11.0 mm, the synchronous reactance of the permanent magnet synchronous machine was computed to be 0.6 pu, and the usage of permanent magnet material to 1247 kg at minimum, in case of the desired input parameters. In this machine, the height of the surface mounted magnets were 35.3 mm, distributed in 12 poles.

It has been observed possibilities for reduction in both mass and size by redesign to a permanent magnet synchronous machine, the former in greatest extent. The machine efficiency was also raised in case of the permanent magnet synchronous machine, from 97.6 to 98.0 %.

Sammendrag

Denne masteroppgaven er en mer gjennomgående studie av det som ble påbegynt i spesialiseringsprosjektet, høsten 2014. Hovedmålet har vært å utvikle og designe en permanentmagnet synkronmaskin for bruk i vannkraftverk. I denne studien har et analytisk designverktøy blitt utviklet for dette formålet. Programmet har blitt skrevet i Matlab. Det analytiske beregningsprogrammet har blitt verifisert med FEM-analyse for drift av maskin i tomgang. Designverktøyet er funnet å ha tilstrekkelig nøyaktighet for denne studien.

Det har blitt utført en litteraturstudie, som har dannet grunnlaget for utviklingen av programmet. De relevante ligningene finnes i den teoretiske delen av denne oppgaven. Det har blitt foretatt et redesign av en 18 MVA synkronmaskin med feltviklinger, der rotoren er byttet ut med en permanentmagnetrotor. Statorens indre diameter ble holdt konstant på 3,51 m for de simulerte maskinene. Etter at luftgapet ble redusert til å være 11,0 mm, fikk denne maskinene en synkronreaktans på 0,6 pu. Totalt ble den nødvendige mengden permanentmagnetmateriale beregnet til 1247 kg, fordelt på de 12 polene. Magnethøyden var på 35.3 mm.

Det har blitt observert at det er mulig å både redusere maskinens totale volum og masse ved et redesign. Reduksjon i masse, vil forholdsvis være mye større enn reduksjon i volum. Permanentmagnetmaskinen fikk en økt virkningsgrad fra 97,6 til 98,0 %, sammenlignet med maskinen med feltviklinger.

Contents

Problem description	I
Preface	III
Abstract	V
Sammendrag	VII
List of symbols	XV
1 Introduction	1
1.1 Background	1
1.2 Objectives	1
1.3 Limitations	2
2 Theoretical background	3
2.1 Generic theory of synchronous generators	4
2.2 Magnetic modelling	5
2.3 Dimensioning process of the PM	5
2.3.1 Carter factor	5
2.3.2 Magnetic circuit model	6
2.3.3 Dimensions of magnets	9
2.3.4 Leakage flux	11
2.3.5 Flux densities in the machine parts	11
2.3.6 Remanent flux density	13
2.4 Inductances	13
2.4.1 Magnetizing inductance	14
2.4.2 Leakage inductance	14
2.5 Losses	15
2.5.1 Losses in permanent magnets	15
2.5.2 Other losses	15
2.6 Main dimensions and parameters in machine design	17
2.6.1 Machine constant	18
2.6.2 Equivalent core length	19
2.6.3 Air gap	19

3	Method and design tools	21
3.1	GenProg	21
3.2	GenProg2	21
3.2.1	Essential modifications in the new version	22
3.3	COMSOL Multiphysics	23
4	Simulations	25
4.1	Input design parameters	25
4.1.1	Stator design	26
4.1.2	Power factor	26
4.2	Output results	27
4.2.1	Validation of the analytical model	27
4.2.2	Permanent magnet rotor design	30
5	Discussion	33
5.1	Validity of the analytical results	33
5.2	The PM rotor design	34
6	Conclusion	37
7	Recommendations for further work	39
	Bibliography	41
	Appendix	42
A	Initialization of GenProg	43
B	Relevant tables	45
C	Input and output for the rotor design	49
C.1	Input machine 2.1	50
C.2	Output machine 2.1	52
C.3	Input machine 2.2	56
C.4	Output machine 2.2	58
C.5	Input machine 2.3	62
C.6	Output machine 2.3	64
C.7	Input machine 2.4	68
C.8	Output machine 2.4	70
D	Attached files	75

List of Figures

2.1	Principle design of PM rotor	3
2.2	Round rotor synchronous generator	4
2.3	The flux path and flux squeezing at the tooth base	5
2.4	Principle linear structure of PM machine	6
2.5	Magnetic circuit model	7
2.6	Circular-arc straight-line permeance model	8
2.7	Arc segment of PM for one pole, with inner and outer radius.	10
2.8	Air gap flux densities over one single PM	13
2.9	Main dimensions of the cross-section	17
3.1	Flowchart of design process in GenProgv2	22
3.2	Arc segment simulated in Comsol	23
4.1	Phasor plot for visualization of over-voltage in no-load operation	27
4.2	Flux density distribution for two poles according to case 1.2.	29
4.3	Arrow plot to visualize flux path	29
4.4	Plot of normalized air gap flux close to the magnets	30
4.5	Reduced harmonics in percent of the fundamental component.	32

LIST OF FIGURES

List of Tables

- 2.1 Permitted values of current 18
- 2.2 Permitted flux densities 18

- 4.1 Design parameters 25
- 4.2 Parameters constraints 26
- 4.3 Stator slots and connection of windings 26
- 4.4 Comparison of analytical and FEM results 28
- 4.5 Comparison of analytical and FEM results at different diameters . 28
- 4.6 Complementary analytical parameters 28
- 4.7 Results for the different machines 31

- B.1 Magnet characteristics 45
- B.3 Permeance factors of the end windings 46
- B.4 Magnet characteristics 46
- B.2 Slot alternatives 47

List of symbols

Symbol	Description
A	linear current density [A/m]
B	magnetic flux density [T]
B_r	remanent flux density [T]
B_{yr}	magnetic flux density in rotor yoke [T]
B_{ys}	magnetic flux density in stator yoke [T]
B_δ	air gap flux density [T]
b	width [m]
b_d	tooth width [m]
b_s	stator slot width [m]
b_v	width of ventilation duct [m]
C	machine constant [kVA/m^3]
C_ϕ	flux concentration factor $[-]$
D_s	inner diameter of the stator [m]
D_r	rotor diameter [m]
E	electromotive force (emf) [V]
f	frequency [f]
H	magnetic field strength [A/m]
h	height [m]
h_d	tooth height [m]
h_{PM}	permanent magnet height [m]
h_s	stator slot height [m]
h_{yr}	rotor yoke height [m]
h_{ys}	stator yoke height [m]
I	electric current [A]
J	current density [A/m^2], moment of inertia [kgm^2]
k_C	Carter factor $[-]$
k_d	distribution factor $[-]$
k_{Fe}	space factor for iron $[-]$
k_{ml}	leakage factor $[-]$
k_w	winding factor $[-]$
L	self-inductance [H]
L_d	tooth inductance [H]
L_m	magnetizing inductance [H]

LIST OF TABLES

L_u	slot leakage inductance [H]
L_{sq}	skew leakage inductance [H]
L_w	end winding leakage inductance [H]
L_δ	air gap leakage inductance [H]
L_σ	leakage inductance [H]
l	length [m]
l'	effective core length [m]
l_b	gross length (of iron core) [-]
m	number of phases [-], mass [kg]
N_s	number of turns in series per phase [-]
n	rotational speed [rpm], rotational frequency [$1/s$]
n_u	number of turns per coil [-]
n_v	number of ventilation ducts [-]
P	active power, losses [W], permeance [H]
P_c	permeance coefficient [H]
p	number of pole pairs [-]
Q	number of slots [-]
q	number of slots per pole per phase [-]
R	electric resistance [Ω]
R_m	magnetic reluctance [$A/Vs = 1/H$]
r	radius [m]
S	apparent power [VA], cross-sectional area, surface area [m^2]
U_m	magnetic voltage [A]
V	electric voltage [V], volume [m^3]
v	speed, velocity [m/s]
w	width [m]
x	reactance [Ω]
α_{PM}	relative pole pitch/magnet width [rad], [$^\circ$]
δ	air gap length [m]
δ_e	equivalent air gap length [m]
δ_{ef}	effective(magnetic) air gap length [m]
δ_0	minimum air gap length [m]
δ_g	power (or rotor) angle with respect to the terminal voltage [rad]
ϵ_{ad}	additional factor magnetic voltage drop [-]
η	efficiency [-], magnet-to-rotor leakage factor [-]
Θ	current linkage [A]
κ	factor for reduction of slot opening [-]
λ	magnet-to-magnet leakage factor [-]
μ	magnetic permeability [H/m]
μ_r	relative magnetic permeability [-]
μ_0	magnetic permeability of vacuum [H/m]
ρ	resistivity [Ωm], density [kg/m^3]
σ	leakage factor [-], conductivity [S/m]
τ_p	pole pitch [m]

τ_u	slot pitch [<i>m</i>]
Φ	magnetic flux [<i>Wb</i>]
Ψ	magnetic flux linkage [<i>V s</i>]
Ω	mechanical angular velocity [<i>rad/s</i>]
ω	electric angular velocity [<i>rad/s</i>]

Abbreviations, sub- and superscripts

Symbol	Description
$\hat{}$	peak value
1	fundamental component
a	armature
AC	alternating current
ad	additional
c	conductor
Cu	copper
d	tooth, direct
DC	direct current
e	equivalent
ef	effective
f	field, spacer between magnets
Fe	iron
FEM	finite element method
max	maximum
min	minimum
mm	magnet-to-magnet
mr	magnet-to-rotor
N	rated
n	nominal, normal
n/a	not available
p	pole
PM	permanent magnet
PMSM	permanent magnet synchronous machine
pu	per unit
r	rotor, runaway(speed)
RMS	root mean square
s	stator
SM	synchronous machine
sat	saturation
tot	total
u	slot
w	end winding
yr	rotor yoke
ys	stator yoke

Chapter 1

Introduction

In this chapter, the problem that is addressed in the study will be introduced. In addition, some motivation for solving it, the objectives and limitations will be presented.

1.1 Background

Pumped storage may be needed to integrate new renewable energy production as large-scale wind-power and small-scale hydropower. The pumped storage hydropower plant can provide energy balance and assist in system stabilization. Alternative designs of the electrical machine in such an application may be expedient. PM synchronous machines may be used instead of traditional synchronous machines with field windings in combination with a power electronic soft-starter, in the power range of 5-20 MW. Due to the redesign by use of permanent magnets, the construction may be simplified and it is possible that the machine will require less space.

Through the 20th century, and into the 21st, the development of permanent magnets have been significant. Especially the introduction of rare-earth permanent magnets in high performance applications have been interesting, due to a high energy product and remanence. Neodymium magnets holds the best specification suitable for this study.

1.2 Objectives

In this study, the following will be the main objectives:

- Develop an analytical design tool for surface mounted PMSM by use of a Matlab script. The analytical procedure will be presented by the equations relevant to the PM rotor design;
- Verify the analytical design tool by simple FEM simulations in no-load operation;

- Propose a redesign of a synchronous machine with field windings, by use of a PM rotor.

1.3 Limitations

The following limitations are applicable in this study:

- Losses in the permanent magnets are disregarded;
- Considerations due to cost will not be treated, regardless it is of interest to minimize the amount of permanent magnet material needed;
- Only non-salient rotor designs with surface mounted PM are treated;
- The design will be based on generator mode of operation only, hence the motor mode of operation will not be treated;
- The base of the stator will be kept constant throughout the study, thus the number of slots, in addition to the layout of windings will not be varied;
- The number of poles and the power rating are also kept constant.

Chapter 2

Theoretical background

Initially, the specialization project [1] accomplished the fall of 2014, should provide the necessary literature survey for this master thesis. Due to some changes in scope during both the specialization project and the master thesis, a complementary literature survey was carried out related to the master thesis. The literature survey is the base for the following presentation of theory associated with PMSM design, focusing on the rotor equipped with surface mounted magnets.

Relevant theory of stator and its windings, permanent magnets and PMSM topologies will not be treated in depth in this thesis, but can be found in the specialization project [1].

Figure 2.1 represents the two principle designs of PMSM rotors, where figure 2.1 (a) will be treated in this thesis.

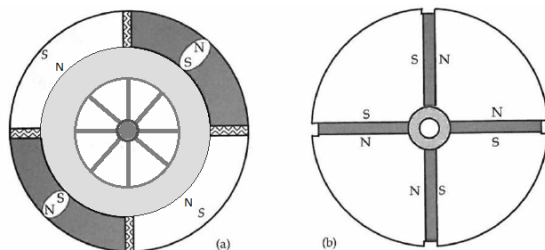


Figure 2.1: Principle PM rotor design: (a) surface mounted PM; (b) interior PM [3].

2.1 Generic theory of synchronous generators

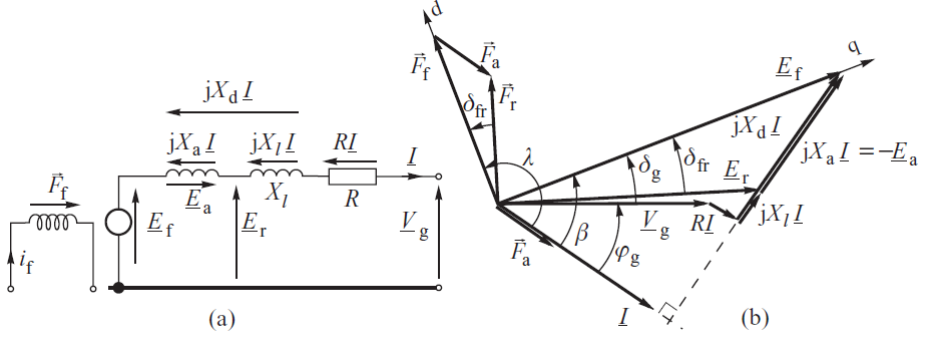


Figure 2.2: Round rotor synchronous generator: (a) equivalent circuit diagram; (b) phasor diagram at lagging power factor [8].

Figure 2.2 is describing a synchronous generator with field windings. Still, this will also be valid in case of a PMSM, except that the field winding to the left in the figure does not exist in such a machine. The subscript denoting the field winding should be replaced by PM, as E_{PM} instead of E_f [2].

As seen in figure 2.2, the air gap emf can be expressed as

$$\underline{E}_r = \underline{E}_{PM} + \underline{E}_a = \underline{E}_{PM} - jX_a \underline{I} \quad (2.1)$$

where \underline{E}_{PM} is the internal emf with magnitude E_{PM} as described in equation (2.3). \underline{E}_a correspond to the armature reaction emf, resulting from a reactance drop due to the armature current [8]. According to figure 2.2, there will also be voltage drops due to the armature winding resistance, in addition to the leakage reactance. The leakage reactance is described through the leakage inductance in section 2.4. Finally, the terminal voltage can be determined by

$$\underline{V}_g = \underline{E}_{PM} - jX_a \underline{I} - jX_l \underline{I} - R \underline{I} = \underline{E}_{PM} - (R + X_d) \underline{I} \quad (2.2)$$

where X_d is the synchronous reactance. The no-load air gap emf is given by the flux linking the armature windings, as derived by Faraday's law of induction [2], and is expressed as

$$E_{PM} = \sqrt{2} \pi f \hat{\phi}_1 N k_w \quad (2.3)$$

The power generated is given by

$$P = \frac{E_{PM} V_g}{x_d} \sin(\delta_g) \quad (2.4)$$

and do not include any reluctance power, which will be present in salient-pole SM [8].

2.2 Magnetic modelling

Magnetic modelling can be based on the analysis of the magnetic flux density and the magnetic field strength in different parts of the machine [2]. The machine will typically have the same number of flux paths as its number of poles [1] [2]. From Ampere's law, the magnetomotive MMF relates to the current linkage

$$MMF = \oint \mathbf{H} \cdot d\mathbf{l} = \sum i = Ni = \Theta \quad (2.5)$$

In the theory of magnetic modelling, the concept of magnetic circuit models is used. An analogy to electric circuits is common, where equation (2.6) is analogous to Ohm's law [3].

$$U = MMF = \phi R \quad (2.6)$$

where U represent the magnetic voltage which equals the MMF . R and ϕ represent the magnetic reluctance and the magnetic flux, respectively. The magnetic conductivity, known as the permeance relate to the reluctance, as follows

$$P = \frac{1}{R_m} = \frac{\mu S_m}{l} \quad (2.7)$$

where S_m is the cross-sectional area of the material, l is the length and μ is the permeability.

2.3 Dimensioning process of the PM

PM synchronous machines are excited by permanent magnets instead of field windings, as in traditional hydropower machines. In the traditional machines, the field windings provide a certain current linkage, as described in equation (2.5), due to the number of turns and the field current. In case of PM machines, the height h_{PM} of the permanent magnet will magnetize the machine at a certain level, at a specific magnet area S_{PM} .

2.3.1 Carter factor

In electrical machines, the stator surface will often be split by slots. This can also be present on the rotor, especially if the machine is equipped with damper bars. The slotting will affect the flux by a decrease in flux density at the slot opening, which will make a local minimum of the air gap flux [2]. Due to Carter's principle, this make the effective air gap longer than the physical air gap as seen in equation (2.8). As

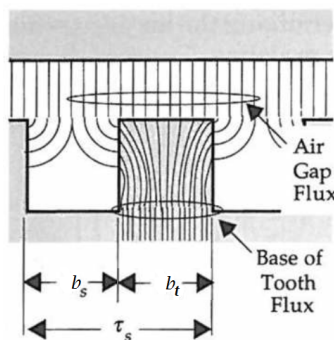


Figure 2.3: The flux path and flux squeezing at the tooth base [3].

seen in figure 2.3, the effective air gap will be longer as the flux path is longer due to the flux squeezing into the tooth.

$$\delta_e = k_C \delta \quad (2.8)$$

where the Carter factor is defined as

$$k_C = \frac{\tau_u}{\tau_u - \kappa b_1} \quad (2.9)$$

where

$$\kappa = \frac{\frac{b_1}{\delta}}{5 + \frac{b_1}{\delta}} \quad (2.10)$$

and b_1 is the slot width.

It exists several approximations of the Carter factor. Regardless, it is important that the Carter factor is calculated on the base of the experienced air gap of the machine. In case of surface mounted PM synchronous machines, the height of the permanent magnet will act as a part of the air gap due to the low permeability of rare earth magnets [3]. The relative permeability, $\mu_r \approx 1$, as for air. The air gap is treated more in depth in section 2.6.3.

2.3.2 Magnetic circuit model

In figure 2.4, a small principle part of the permanent magnets including the flux flowing in the rotor and stator back iron is presented. This sketch represents three magnetic poles linearly, and it should be noted that in a real electrical machine this will follow the curvature of the stator.

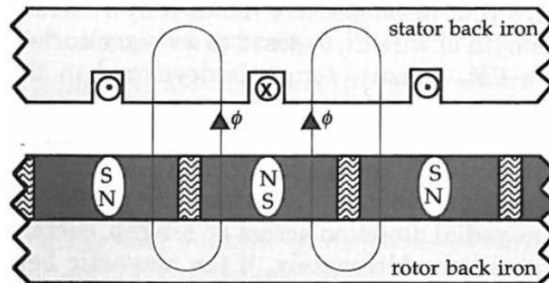


Figure 2.4: Principle linear structure of PM machine, including the flux path [3].

The magnetic circuit model of one single flux path of figure 2.4 is given in figure 2.5. In figure 2.5, the notation of the $\phi/2$ is used, based on the fact that the air gap flux invariably has contribution from two magnets.

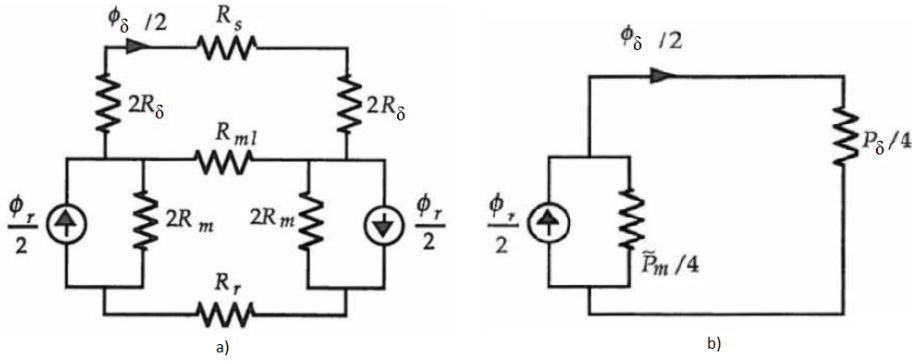


Figure 2.5: (a) Magnetic circuit model (b) Simplification of circuit model [3].

Analytical model

From the circuit model given in figure 2.5 (b), the following expression can be written

$$\frac{\phi_\delta}{2} = \frac{\frac{P_\delta}{4}}{\frac{P_\delta}{4} + \frac{\tilde{P}_{PM}}{4}} \frac{\phi_r}{2} \quad (2.11)$$

which can be simplified to

$$\phi_\delta = \frac{1}{1 + \frac{\tilde{P}_{PM}}{P_\delta}} \phi_r \quad (2.12)$$

where the combination of the magnet permeance and the magnet leakage permeance can be expressed

$$\tilde{P}_{PM} = P_{PM} + 4P_{ml} \quad (2.13)$$

The concentration factor is defined as

$$C_\phi = \frac{S_{PM}}{S_\delta} \quad (2.14)$$

respectively based on the air gap surface area of the permanent magnet

$$S_{PM} = \alpha_{PM} \tau_p l_b \quad (2.15)$$

and the area of the air gap

$$S_\delta = \frac{\tau_p l_b (1 + \alpha_{PM})}{2} \quad (2.16)$$

This area is a representation of the air gap area per pole and approximates an average value. The cross-sectional area where the flux is flowing is increasing at increasing diameter, when approaching the stator.

Further the magnet leakage factor is

$$k_{ml} = 1 + \frac{4h_{PM}}{\pi\mu_r\alpha_{PM}\tau_p} \ln \left(1 + \pi \frac{\delta}{(1 - \alpha_{PM})\tau_p} \right) \quad (2.17)$$

A low magnet leakage flux will result in a higher performance of the machine. The closer k_{ml} is to 1, the better [3].

The permeance coefficient is defined as

$$P_c = \frac{h_{PM}}{\delta C_\phi} \quad (2.18)$$

which is essential of calculating the air gap flux density as described in equation (2.19).

Finally, the relation between the air gap flux density and the remanent flux density can be expressed as

$$B_\delta = \frac{C_\phi}{1 + \frac{\mu_r k_C k_{ml}}{P_c}} B_r \quad (2.19)$$

Improved analytical model of air gap leakage flux

The improved model has the same basis as the analytical model as presented. In addition, the improved model includes a more detailed description of the leakage flux. Now the magnet-to-rotor leakage flux is taken into account, not only the magnet-to-magnet leakage flux. This approach will be described briefly, but all equations that are relevant to perform the calculations will be presented. Still the circular-arc straight-line permeance model is used, as expressed in equation (2.17) and visualized in figure 2.6.

Each leakage flux is described by a reluctance which is related to a leakage factor [11].

$$\eta = \frac{R_m}{R_{mr}} = \frac{h_{PM}}{\pi\mu_r w_m} \ln \left(1 + \frac{\pi\delta_e}{h_{PM}} \right) \quad (2.20)$$

$$\lambda = \frac{R_m}{R_{mm}} = \frac{h_{PM}}{\pi\mu_r w_m} \ln \left(1 + \frac{\pi\delta_e}{w_f} \right) \quad (2.21)$$

where R_m is the magnet reluctance, w_m is the magnet width and w_f is the gap between the magnets.

The average air gap flux density can be expressed by

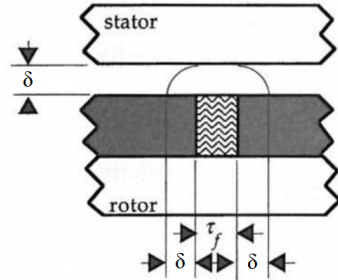


Figure 2.6: Circular-arc straight-line permeance model describing magnet-to-magnet leakage flux [3].

$$B_{\delta,ave} = \left[1 + \frac{w_f}{w_m} + \mu_r \frac{\delta_e}{h_{PM}} \frac{w_m + w_f}{w_m + 2\delta_e} (1 + 2\eta + 4\lambda) \right]^{-1} B_r \quad (2.22)$$

The air gap leakage factor describes the ratio between the average air gap flux and the flux within the magnet.

$$K_{L\delta} = \frac{\Phi_{\delta}}{\Phi_m} = \left[1 + \mu_r \frac{\delta_e}{h_{PM}} \frac{w_m}{w_m + 2\delta_e} (2\eta + 4\lambda) \right]^{-1} \quad (2.23)$$

2.3.3 Dimensions of magnets

The air gap surface area of each permanent magnet is given by equation (2.15). Further, the total length of the magnet will equal the gross iron length of the machine. The height of the permanent magnet is found by iteration of equation (2.22), until the desired air gap flux density is reached.

This iteration process do only include the reluctance of the air gap. There are other reluctances, which also contribute to the magnetic voltage drop, as described in [2]:

$$MFF = U_m = 2U_{m\delta} + 2U_{m,ds} + U_{m,ys} + U_{m,yr} \quad (2.24)$$

including magnetic voltage drop in stator teeth, stator yoke and rotor yoke. By considering the ratio between the voltage drop over the air gap and the other machine parts, an additional factor can be determined

$$\epsilon_{ad} = \frac{2U_{m,ds} + U_{m,ys} + U_{m,yr}}{2U_{m\delta}} \quad (2.25)$$

According to [2] and use of the Matlab tool GenProg described in [5] and [6], the value of ϵ can be about 3 %. To take the effect of saturation into account, approximately 10 % can be added to the magnet height [7]. Then a new height of the magnet can be calculated

$$h'_{PM} = h_{PM} \cdot (\epsilon_{ad} + 1) \cdot 1.1 \quad (2.26)$$

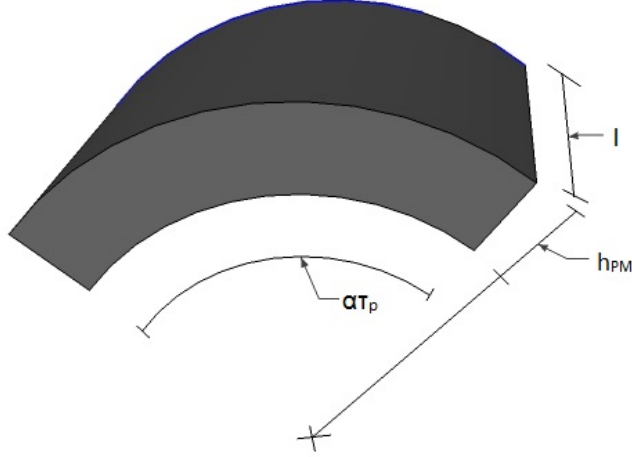


Figure 2.7: Arc segment of PM for one pole, with inner and outer radius.

Volume of magnet

The volume of the magnet is calculated out from the geometric shape displayed in figure 2.7. The outer radius of the magnet is calculated by subtracting the length of the air gap from the stator bore radius

$$r_o = \frac{D_r}{2} = \frac{D_s}{2} - \delta_0 \quad (2.27)$$

and the inner radius of the magnet is

$$r_i = \frac{D_{ry}}{2} = r_o - h_{PM} \quad (2.28)$$

which also equals the radius of the rotor yoke, $D_{ry}/2$. The cross-section area of a single magnet can then be calculated as

$$S_{PM,axial} = \frac{\alpha_{PM}\pi(r_o^2 - r_i^2)}{2p} \quad (2.29)$$

Finally, the volume of each single magnet can be calculated

$$V_{PM} = S_{PM,axial} \cdot l_b \quad (2.30)$$

To find the total volume of permanent magnet material, V_{PM} have to be multiplied with the number of poles, $2p$.

Moment of inertia

Generally, the moment of inertia for a point mass rotating around an axis can be expressed by

$$J = mr^2 \quad (2.31)$$

where m is the point mass and r is the distance to the axis of rotation. A rotating part in the machine will not be a point mass, but a simplification is made by using an equivalent average value of the distance to the axis of rotation. In an electrical machine, all rotating parts will contribute to the moment of inertia of the machine. The most important contribution, in addition to the permanent magnets, will be the rotor ring.

2.3.4 Leakage flux

The leakage flux consists of several components, mainly divided into components that are crossing the air gap and not crossing the air gap. In surface mounted machines, the air gap leakage flux consists of the magnet-to-magnet flux and magnet-to-rotor-yoke flux [11].

2.3.5 Flux densities in the machine parts

The following flux densities are calculated for a no-load situation. Generally, the nominal flux densities can be calculated by taking the air gap emf into account. The air gap emf is also known as the relative induced voltage, E_r [7]. E_r is explained deeper in section 2.1 on page 4.

$$B_{nominal} = E_r \cdot B_{no-load} \quad (2.32)$$

Equation (2.32) originates from field winding SM theory. Since the excitation in a PMSM is fixed, it is expected that the machine will run on over-voltage at the terminals in a no-load situation.

The maximum of the flux density of the stator yoke can be calculated at the q-axis. At this point, the air gap flux density is zero, and half of the main flux will flow through the stator yoke.

$$\hat{B}_{ys} = \frac{\hat{\Phi}_m}{2S_{ys}} = \frac{\hat{\Phi}_m}{2k_{Fe}l'h_{ys}} \quad (2.33)$$

where S_{ys} is the area of the stator yoke, k_{Fe} is the space factor of iron and h_{ys} is the height of the yoke. l' is describing the equivalent length of the machine, which is described in section 2.6.2 on page 19.

In the same way the maximum flux density of the rotor yoke can be calculated

$$\hat{B}_{yr} = \frac{\hat{\Phi}_m}{2S_{yr}} = \frac{\hat{\Phi}_m}{2k_{Fe}l'h_{yr}K_{L\delta}} \quad (2.34)$$

The flux density of the teeth can be expressed as

$$\hat{B}_d = \frac{\hat{\Phi}_d}{S_d} = \frac{\hat{\Phi}_d}{k_{Fe}l'} \cdot \frac{1}{b_d(h)} \quad (2.35)$$

since the area of a tooth will be increasing at increasing diameter of the machine. This implies that the flux density of a tooth will be at its maximum close to the air gap. The tooth width is given by

$$b_d(h) = b_{d,min} + \left(\frac{b_{d,max} - b_{d,min}}{h_s} \right) \cdot h \quad (2.36)$$

Generally, the flux density in the teeth will be high. This can cause some saturation in the teeth, which can be solved graphically by the BH-curve of the core material [2].

The air gap flux density is already given by equation (2.19). Still, to define the wanted air gap flux, a diversion of equation (2.3) have to be used.

$$\hat{B}_\delta = k_m \cdot \frac{\hat{\Phi}_m}{\tau_p l} \quad (2.37)$$

The relation between the flux and the flux density can also be derived through a surface integral for one pole. This is described for a cosinusoidal air gap flux density where k_m equals $\pi/2$ [2]. The peak value of the flux, $\hat{\Phi}_m$ is found by

$$\hat{\Phi}_m = \frac{U_n}{4\sqrt{3}k_f k_w N_s} \quad (2.38)$$

k_m is the factor between the maximum air gap flux density \hat{B}_δ and the mean fundamental flux density in no-load, and have the value of 1.515 [7]. As seen in figure 2.8, the different air gap flux densities are represented, where the area under each graph is identical. k_w is the winding factor described in [1]. The form factor k_f is set to be 1.11 [7].

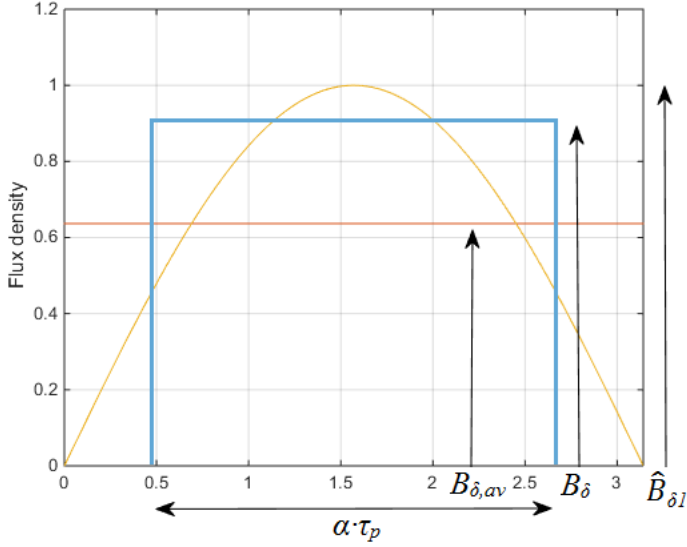


Figure 2.8: Air gap flux densities over one single PM

2.3.6 Remanent flux density

Neodymium as a rare earth magnet perform the best values of the magnetic remanence [2]. Typically, the remanence is within the range of 1.03-1.3 T. In this thesis the remanent flux density is assumed to be 1.2 T. The performance of the neodymium magnets are strongly depending on the temperature, and can be described by a reference remanence at 20 °C, and a temperature coefficient.

$$B_r(T) = B_{r,20^\circ C} + \alpha_T(T - 20) \quad (2.39)$$

where α_T equals -0.12 %/°C, which is found in table B.1. If the permanent magnet is operating at a temperature of 70 °C, then the actual remanence will be 1.14 T, when $B_{r,20^\circ C}$ equals 1.2 T.

2.4 Inductances

The direct-axis synchronous inductance consists of the contribution of both the direct-axis magnetizing inductance and the leakage inductance

$$L_d = L_{md} + L_\sigma \quad (2.40)$$

The magnetizing inductance represents the fundamental harmonic component of the air gap inductance, whereas the residual components contribute to the air gap leakage inductance [2].

If the machine is operating at a constant frequency, the synchronous inductance will relate proportionally to the synchronous reactance [2]

$$X_d = \omega L_d \quad (2.41)$$

2.4.1 Magnetizing inductance

The magnetizing inductance is given by

$$L_m = \frac{mD_s}{\pi p^2 \delta_{ef}} \mu_0 l' (k_{ws1} N_s)^2 \quad (2.42)$$

where δ_{ef} is the effective air gap formed by both the physical air gap in interaction with the height of the permanent magnets. This is also known as the magnetic air gap, as described in section 2.6.3 on page 19. Since the scope of this thesis is of non-salient synchronous machines, the magnetizing inductance will be the same in both the d- and q-axis [2].

Compared to field winding machines, the magnetizing inductance will be relatively small due to the large length of the effective air gap.

2.4.2 Leakage inductance

There are several components contributing to the winding self-inductance, due to (co)energy stored in four distinct areas [3]. These are the back iron, the air gap, the slots and the end turns. The inductance due to the magnetic field in the back iron is insignificant, because of its relatively high permeability. The permanent magnets generate flux independent of the current in the stator windings. Hence, these will not contribute to the self-inductance.

The total leakage inductance can be expressed as a sum by

$$L_\sigma = L_\delta + L_u + L_w \quad (2.43)$$

The air gap inductance of one single coil is given in terms of

$$L_\delta = \frac{n_u^2 \mu_r \mu_0 l \tau_p}{2(h_{PM} + \mu_R \delta_e)} \quad (2.44)$$

To find the total air gap leakage inductance related to equation (2.44), L_δ have to be multiplied by the total number of turns per phase, N_s [3]. The parameter, n_u , represent the number of turns per coil. By use of Roebel bars, only a single effective turn per coil will be present [2].

The slot leakage inductance is expressed as

$$L_u = \left(\frac{n_u^2}{3} \right) \frac{\mu_0 h_s l}{b_s} \quad (2.45)$$

where the factor of one third appears because the magnetic field is increasing linearly, rather than being constant in the whole slot height.

When the end turn leakage inductance is regarded, the structure of the winding have to be taken into account [2].

$$L_w = \frac{4m}{Q} q N_s^2 \mu_0 l_w \lambda_w \quad (2.46)$$

where

$$l_w = 2l_{ew} + W_{ew} \quad (2.47)$$

and

$$l_w \lambda_w = 2l_{ew} \lambda_{l_{ew}} + W_{ew} \lambda_W \quad (2.48)$$

The permeance factors $\lambda_{l_{ew}}$ and λ_w are corresponding to different end winding structures, which can be found in table B.3 on page 46.

2.5 Losses

In the machine parts, different categories of losses will be present. The losses will be described briefly in this section.

2.5.1 Losses in permanent magnets

In a PMSM, there will be no losses associated with field windings, since no windings in the rotor are present. On the other hand, the PMSM introduces losses in the magnet itself. Due to the relatively good conductivity of neodymium magnets, eddy currents can be induced in the magnet [2][9][12].

The formation of the eddy currents can be described by Faraday's law of induction [2][12].

$$\int \mathbf{E} \cdot d\mathbf{l} = \int \frac{\mathbf{J}}{\sigma} \cdot d\mathbf{l} = -\frac{\partial \Phi}{\partial t} \quad (2.49)$$

Variation in the air gap flux can be caused by the stator slots, especially due to a design including open slots. The harmonic content of the air gap flux can induce currents in the permanent magnets.

It is also stated that hysteresis losses will be present in the magnets at high frequencies of AC field due to the slot ripple [10].

2.5.2 Other losses

Copper losses

The copper losses will only occur in the stator windings in PM machines, since there are no rotor field windings present. Generally, the DC resistance is described by

$$R_{DC} = \frac{l_c}{\sigma_c a S_c} \quad (2.50)$$

where l_c is the length of the conductor, σ_c is the conductivity for the material which in this case is copper, a is the number of parallel paths in the windings, and S_c is the cross-sectional area.

In calculation of the copper losses, the losses are divided into DC and AC losses, where the AC losses include the skin effect [2]. Further, the stator windings are assumed made by Roebel bars. By use of these bars, the layers in the winding are revolved periodical [2]. In this way, the skin effect is minimized, since the sum of partial fluxes in the integration paths, causing eddy currents, are eliminated.

Iron losses

The iron losses can be found by dividing the magnetic circuit into n sections, where the flux density will be approximately constant. This implies that the iron losses can be calculated individually for the stator yoke, stator teeth and rotor yoke [2].

$$P_{Fe} = \sum_n k_{Fe,n} P_{10} \left(\frac{\hat{B}_n}{1[T]} \right)^2 \cdot m_{Fe,n} \quad (2.51)$$

where k_{Fe} is a coefficient including saturation in the iron, which have the values of 1.5-1.7 for the stator yoke, and 2 for the teeth. P_{10} is the loss in W/kg given by the manufacturer at 1 [T].

Mechanical losses

Mainly, the mechanical losses consist of the windage, bearing friction and ventilator losses. The windage loss is consisting of the power due to the resisting drag torque on the rotor, described by a rotating cylinder, and the end surfaces of the rotor contribute to friction loss, in terms of $P_{\rho w1}$ and $P_{\rho w2}$ respectively [2].

$$P_{\rho w} = P_{\rho w1} + P_{\rho w2} \quad (2.52)$$

where

$$P_{\rho w1} = \frac{1}{32} k C_M \pi \rho \Omega^3 D_r^4 l_r \quad (2.53)$$

and

$$P_{\rho w2} = \frac{1}{64} k C_M \pi \rho \Omega^3 (D_r^5 - D_{ri}^5) \quad (2.54)$$

C_M is the torque coefficient defined for different Reynold numbers, Ω is the mechanical angular velocity, k is a roughness coefficient (for smooth surface $k = 1$, usually $k = 1 - 1.4$). D_r and D_{ri} are the diameters of the rotor and the rotor shaft respectively. l_r is the rotor length.

The bearing friction and ventilator losses do also belong to the mechanical losses. It is complicated to express these losses in a generic and analytical way. Regardless, this is described by empirical equations in [6].

Additional losses

The additional losses are very difficult to calculate and measure. By experience, these losses will be about 0.05-0.2% of the machine power [2]. These losses mainly originate from the eddy current losses in the stator construction [6].

2.6 Main dimensions and parameters in machine design

The area and the height of the PM can be calculated based on the theory presented in section 2.3.2.

When designing an electrical machine, there can be a considerable number of free parameters [2]. Without any limitation of the number of free parameters, the optimization will be extremely complicated. Based on that the variation in the value of numerous of the free parameters will be slight, these can be assumed constant. Then only 8 parameters will be considered as free parameters:

- outer diameter;
- length of the stator stack;
- width of stator slot;
- height of stator slot;
- inner stator diameter;
- air gap length;
- peak value of the air gap flux density;
- pole pair and frequency.

When designing a field winding synchronous machine the height and width of the rotor slots are also considered as free parameters.

In the beginning of the design process, the main dimension have to be selected. These are the air gap diameter D_s , measured at the stator bore, as seen in figure 2.9, in addition to the equivalent core length l' .

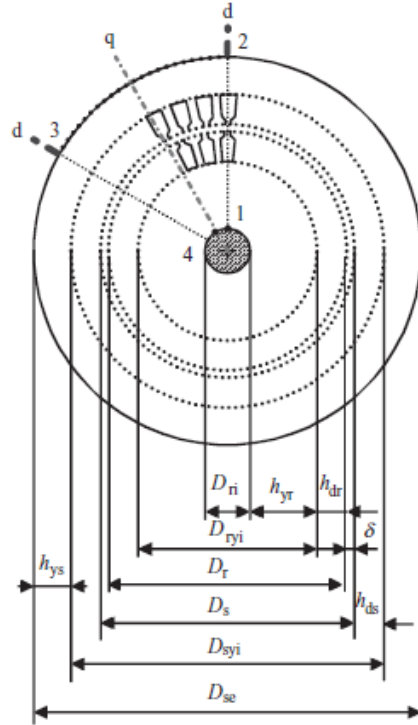


Figure 2.9: Main dimensions of the cross-section [2].

Table 2.1: Permitted values of current in salient-pole SM or PMSM [2]:

Linear current density	35-65	$A/kA/m$
Current density	3.5-6	$J/A/mm^2$

Some empirically defined intervals of variation of the current as well as the flux densities can be found in table 2.1 and 2.2. Next, the insulation and the cooling of the machine are the base of the permitted loading level. In case of PM machines, values of table 2.2 may be chosen in the lower segment of the flux density range. This is caused by the limited remanence of the permanent magnets. In table 2.1, the lower values of the current density J are suitable for larger machines, and the lower values of the linear current density A suitable for small machines [2].

Table 2.2: Permitted flux densities in non-salient synchronous machine [2]:

	Flux density B[T]	
Air gap	$\hat{B}_{\delta 1}$	0.8 - 1.05
Stator yoke	B_{ys}	1.1 - 1.5
Tooth	B_d	1.5 - 2.0
Rotor yoke	B_{yr}	1.1 - 1.7

2.6.1 Machine constant

The machine constant is given by

$$C = \frac{S[kVA]}{D_s^2 \cdot l \cdot n} \quad (2.55)$$

where D is the inner stator diameter, l is the stator length including ventilation channels, and n is the mechanical speed of the machine in rpm [7]. This describes how much power the machine will provide per volume. A typical machine constant for a machine in the range of 10 - 50 MVA, is about 4.5 - 5.5, but can be significantly greater in machines of a higher power rating [7]. One example for increasing the machine constant is to have a more efficient cooling system. This can be provided by integrating water-cooling in the machine.

The machine constant is a result of the following relations [2]

$$S = mE_m I_s = \frac{\pi^2}{\sqrt{2}} k_{ws1} A \hat{B}_\delta D_s^2 l n \quad (2.56)$$

where

$$C = \frac{\pi^2}{\sqrt{2}} k_{ws1} A \hat{B}_\delta \quad (2.57)$$

In equation (2.56) and (2.57), A is the linear current density related to the armature loading and armature current. \hat{B}_δ is the maximum air gap flux density related to the induced voltage.

The linear current density is expressed by

$$A = \frac{I_u}{\tau_s} = \frac{I_u Q_s}{\pi D_s} = \frac{2I_s N_s m}{\pi D_s} \quad (2.58)$$

where I_u is the slot current, I_s is the armature current and N_s is the number of turns in series per phase m .

The maximum air gap flux density is related to the maximum flux penetrating a phase winding

$$\hat{\Phi}_m = \int_S B_\delta dS = l' \tau_p \alpha_{PM} \hat{B}_\delta \quad (2.59)$$

where $\alpha_{PM} \hat{B}_\delta$ equals the average value of the air gap flux density.

2.6.2 Equivalent core length

The gross length of the core of the machine can be calculated through by equation (2.55). To provide air-cooling of the machine, the core can be constructed with radial ventilation ducts [2]. Due to the fringing effect, an edge field may occur at these ventilation ducts, in addition to at the end of the machine.

The edge field at the machine ends can be approximated by an insignificant lengthening of the core length

$$l' \approx l + 2\delta \quad (2.60)$$

Due to the insignificance, the real length provide a sufficient accuracy in calculations. However, the effect of the ventilation ducts have to be taken into account. The equivalent width of the ducts are given through the Carter factor, in the same way as for the air gap.

$$b_{ve} = \kappa b_v \quad (2.61)$$

Then the equivalent length of the machine can be calculated by an approximation

$$l' \approx l - n_v b_{ve} + 2\delta \quad (2.62)$$

where n_v is the number of ventilation ducts.

2.6.3 Air gap

In electrical machine design, the length of the air gap has a substantial impact regarding the machine characteristics [2]. Principally, a small air gap will make the machine easier to magnetize, due to the low permeability of air. On the other hand, a small air gap leads to increased eddy current losses of the rotor and stator

surfaces, caused by the permeance harmonics created by the slots. In addition, current linkage harmonics of the stator increase the surface losses of the rotor, when the air gap is small. No theoretical optimum has been solved for the air gap length. Hence, empirical equations are used to calculate a suitable length.

When defining the air gap, the permitted armature reaction is essential. The flux caused by the armature reaction should not reduce the air gap flux density in too great extent. To assure this requirement the current linkage of the permanent magnets have to be greater than the current linkage of the armature

$$\Theta_{PM} \geq \Theta_a \quad (2.63)$$

For synchronous machines this condition can be rewritten

$$\frac{\hat{B}_\delta}{\mu_0} \delta k_C \geq \frac{1}{2} \alpha \tau_p A_a \quad (2.64)$$

Then the air gap is defined

$$\delta \geq \frac{1}{2} \alpha \mu_0 \tau_p \frac{A_a}{\hat{B}_\delta} = \gamma \tau_p \frac{A_a}{\hat{B}_\delta} \quad (2.65)$$

where the γ coefficients can be found in table B.4 on page 46. In equation (2.65) \hat{B}_δ is set to be $0.9 T$.

As mentioned, it is advantageous to make the physical air gap as small as possible, then the amount of permanent magnet material can be reduced. Still, in higher speed machines, the air gap harmonics may cause very high losses in the permanent magnet material, as well as in the ferromagnetic material below the magnets. To avoid a critical increase in the magnet temperature, the air gap length need to be increased in such cases.

The magnetic air gap of surface mounted magnets machines can be calculated as

$$\delta_{ef} = \frac{h_{PM}}{\mu_{rPM}} + \delta_e \quad (2.66)$$

which will be the experienced air gap of the machine.

The synchronous inductance is a function of the air gap length. Caused by the large magnetic air gap in PM synchronous machines, the synchronous inductance will in most cases be low, and the machine maximum torque high [2].

Chapter 3

Method and design tools

In this chapter, the design programs will be introduced. Firstly, the Matlab program is to be treated. Next, the application, COMSOL, used for the validation will be presented.

3.1 GenProg

In 2010 a Matlab program called GenProg was first made. This is well described and documented in [5] and [6]. Fundamentally, this was made to be an analytic tool to design and optimize synchronous generators for hydropower application. GenProg is reading its input from an Excel file, and writing the calculated results to an output file.

3.2 GenProg2

GenProg2 is a modification of the original calculation program GenProg. Figure 3.1 represents the part of the program that is doing calculations for PM machines. At node 2, the decision is made of which machine type the calculations are to be executed for. If the calculations are chosen to be performed for ordinary synchronous machines with field windings, the design process is exactly as described in [5] and [6]. This implies that the same Excel files for input and output are used, regardless of type of calculation.

A more detailed description of how to use the program can be found in chapter A on page 43.

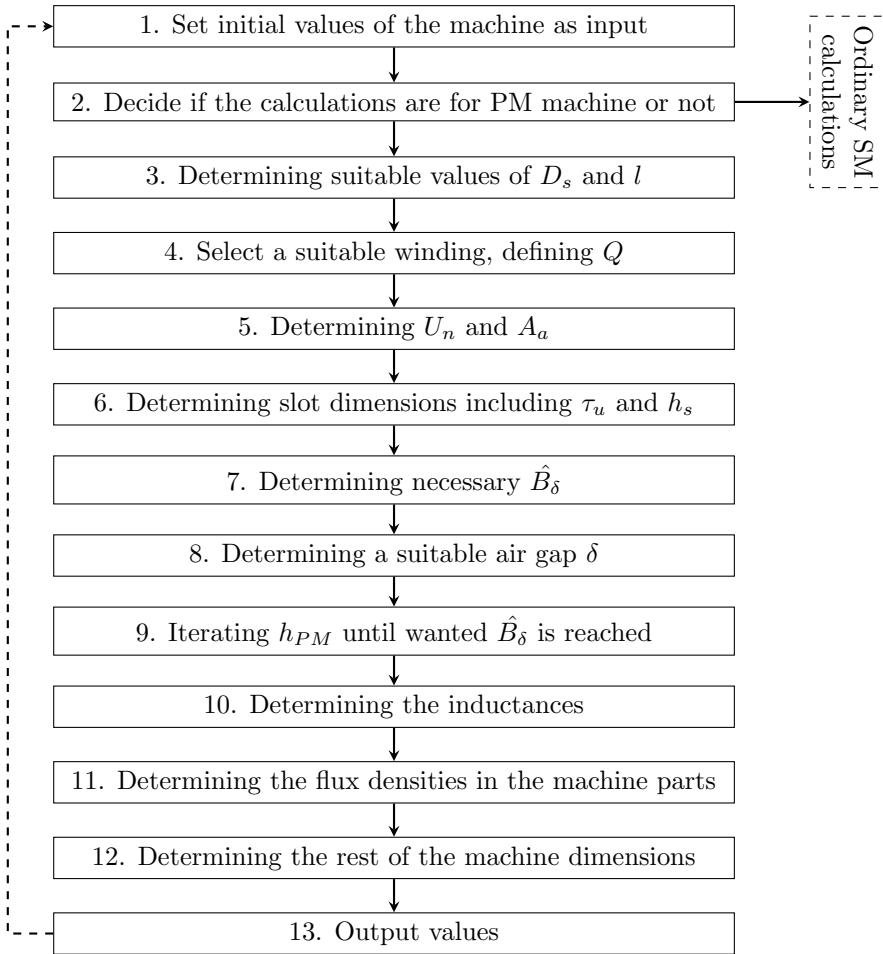


Figure 3.1: Flowchart of design process in GenProgV2.

3.2.1 Essential modifications in the new version

The principal change in the new version is the exchange of the part in the Matlab code, which is describing the rotor. The part, which is including calculations to dimension the field windings, is replaced by equations to perform calculations to dimension the permanent magnets.

Overview of PM program parts:

- Iteration of magnet height;
- Calculation of the other geometric dimensions of the PM;
- Calculation of the inductances;
- Calculation of the phasors and phasor diagram;
- Modification of the relevant mechanical calculations.

In the new version, no calculations of heat flow and temperatures are performed, since the PM loss is not calculated. Some of the other parameters are set to be zero due to the absence of the field windings.

3.3 COMSOL Multiphysics

COMSOL Multiphysics is a FEM analysis tool, which is used in order to evaluate the validity of the analytical Matlab model. All simulations performed in COMSOL are describing a stationary no-load situation. The applied *Physics* are according to *Magnetic Fields, No Currents*. The permanent magnets are set to have a remanent flux density defined by *Magnetic Flux Conservation*, while the *Magnetic Flux Conservation* of iron is described by the BH-curve of the material. At the boundary, which is mirroring the rest of the machine, *Zero Magnetic Scalar Potential* is defined.

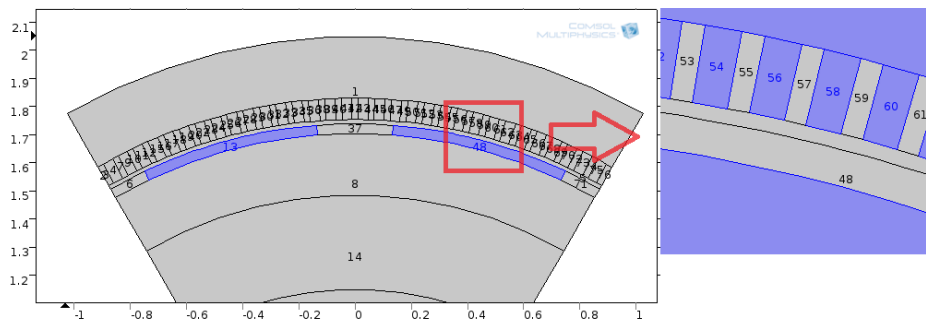


Figure 3.2: Arc segment simulated in Comsol including close-up of air gap, stator teeth and PM.

Chapter 4

Simulations

At first, in this section the base of the calculations will be treated. The base include both some input parameters to be able to design an electrical machine, as well as some constraints of other parameters, which are to be calculated. Second, the output results will be presented.

Table 4.1: Input design parameters:

Description	Parameter	Value
Apparent power	S	18 [MVA]
Electric frequency	f_e	50 [Hz]
Phases	m	3 [#phases]
Poles	$2p$	12 [#poles]
Nominal speed	n	500 [rpm]
Moment of inertia	GD^2	225 [tm ²]
Machine constant	C	5 [-]
Relative pole pitch	α	0.7 [-]
Remanence	$B_{r,20^\circ C}$	1.2 [T]
Slot/tooth ratio	b_s/b_t	0.6 [-]

4.1 Input design parameters

The input parameters according to table 4.1 were set in cooperation with the supervisor. These input parameters are the same for every machine simulated in this study, both in the validation and the rotor design sections. The exception is *Machine 2.4* in the rotor design, where the armature loading was increased, and thus also the machine constant was increased. The machine, which is described in [7], is also used as inspiration due to its suitable size with accordance to the scope of this thesis.

The value of the remanence of the neodymium magnet given in table 4.1 is

1.2 T. It is assumed that the permanent magnets will operate at a temperature about 70 °C. Then the correct remanent flux density will be 1.14 T.

Some constraints were also given, as described in table 4.2.

Table 4.2: Parameter constraints:

Parameter	Value
$x_{d,max}$	1.1 [pu]
$B_{t,max}$	1.8 [T]
$B_{y,max}$	1.2 [T]
$J_{s,max}$	3.5 [A/mm ²]

4.1.1 Stator design

The stator is identical as the stator presented in the specialization project [1]. Thus, the results involving the stator will not be treated in depth, but some important values are presented in table 4.3. In addition, the base of the choice of the number of slots is presented in table B.2 on page 47.

Table 4.3: Stator slots and connection of windings:

	Number
Slots	198
Coil span	14
Turns per coil	1
Parallel circuits	1
Turns per phase	66

4.1.2 Power factor

As seen in figure 4.1, the power factor the machine should be operating at, have to be considered in relation to the tolerated over-voltage at the generator terminals in no-load. Since the PMSM has a constant excitation, the generator has to run at over-voltage in no-load to be able to operate at the rated terminal voltage, V_g , at nominal loading. The over-voltage is remarkable greater at an inductive power factor compared to the unity power factor, both are marked by the stippled lines in the figure. Thus, the over-voltage equals the value of the internal emf, E_{PM} .

In figure 4.1, the phasor plot is describing the exact same machine, where only the power factor is changed.

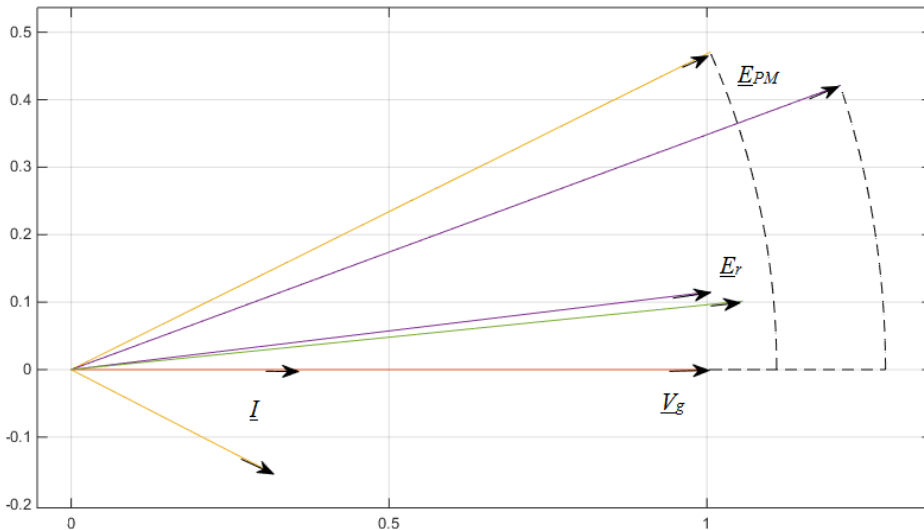


Figure 4.1: Phasor plot for visualization of over-voltage in no-load operation at power factor equal to 0.9 and 1.

4.2 Output results

In this section, the output results are presented. At first, results due to the validation of the analytical Matlab program will be treated through ten different cases. Further, several SM designs will be presented, where four machines will be treated in total.

4.2.1 Validation of the analytical model

To validate the analytical model, FEM analysis was executed. The validation was performed for eight cases with different relative pole pitches α and air gaps δ , while the rest of the dimensions were kept constant. Two additional cases were also simulated, where the stator bore diameter was varied as described in table 4.5. The parameters described in table 4.1 were the input parameters for the simulation.

Values of $B_{\delta,av}$ and B_m obtained from the analytical and the FEM simulation were compared, and a percentage error was calculated in each case. The results are presented in table 4.4.

It has been observed divergence in the iteration of the magnet height for low values of α . For lower values of α than 0.59 at an air gap equal to 15 mm, the analytical simulation tool seem to be useless.

Table 4.4: Comparison of analytical and FEM results, where flux densities are given in $[T]$, $D_s = 3.51 \text{ m}$:

Case	Geom. dim.		Analytical			FEM		Error [%]	
	α	$\delta[mm]$	$h_{PM}[mm]$	$B_{\delta,av}$	B_m	$B_{\delta,av}$	B_m	$B_{\delta,av}$	B_m
1.1	0.6	10.0	70.4	0.563	0.944	0.574	0.969	1.92	2.58
1.2	0.7	10.0	32.0	0.563	0.812	0.573	0.821	1.75	1.10
1.3	0.8	10.0	21.2	0.563	0.713	0.572	0.714	1.57	0.14
1.4	0.9	10.0	16.0	0.563	0.636	0.577	0.639	2.43	0.47
1.5	0.6	15.0	131	0.563	0.947	0.585	1.01	3.76	6.24
1.6	0.7	15.0	49.0	0.563	0.817	0.582	0.843	3.26	3.08
1.7	0.8	15.0	31.5	0.563	0.717	0.583	0.735	3.43	2.45
1.8	0.9	15.0	23.5	0.563	0.641	0.586	0.655	3.92	2.14

The error in table 4.4 and 4.5 is calculated in terms of

$$Error = \frac{FEM \text{ results} - \text{analytical results}}{FEM \text{ results}} \cdot 100\% \quad (4.1)$$

Table 4.5: Additional comparison, where flux densities are given in $[T]$, $D_s = 3.00 \text{ m}$ at case 9 and $D_s = 4.00 \text{ m}$ at case 10:

Case	Geom. dim.		Analytical			FEM		Error [%]	
	α	$\delta[mm]$	$h_{PM}[mm]$	$B_{\delta,av}$	B_m	$B_{\delta,av}$	B_m	$B_{\delta,av}$	B_m
1.9	0.7	12.6	54.9	0.598	0.865	0.620	0.901	3.55	4.00
1.10	0.7	16.8	50.7	0.553	0.802	0.571	0.825	3.15	2.79

Table 4.6 presents values for parameters defined in the theoretical background, treated in section 2.3.2 on page 6. As expected, the leakage flux described through the leakage factor $K_{L\delta}$, is increasing at increasing α and increasing δ . When the leakage flux is increasing, the leakage factor decreases.

The parameters η and λ describe the magnet-to-rotor and magnet-to-magnet leakage flux, respectively.

Table 4.6: Complementary analytical parameters:

Case	Geom. dim.		Analytical			
	α	$\delta[mm]$	η	λ	$K_{L\delta}$	$x_d[pv]$
1.1	0.6	10.0	0.0142	0.0028	0.9933	0.367
1.2	0.7	10.0	0.0102	0.0015	0.9901	0.650
1.3	0.8	10.0	0.0078	0.0012	0.9881	0.851
1.4	0.9	10.0	0.0062	0.0016	0.9855	1.004
1.5	0.6	15.0	0.0219	0.0077	0.9903	0.226
1.6	0.7	15.0	0.0153	0.0033	0.9846	0.446
1.7	0.8	15.0	0.0116	0.0027	0.9812	0.592
1.8	0.9	15.0	0.0092	0.0032	0.9765	0.700

Figure 4.2 shows the flux density distribution of the machine segment simulated in COMSOL. This distribution was the base of the FEM values given in table 4.4, where the average values were calculated through the surface average of the defined areas of the air gap and the permanent magnet.

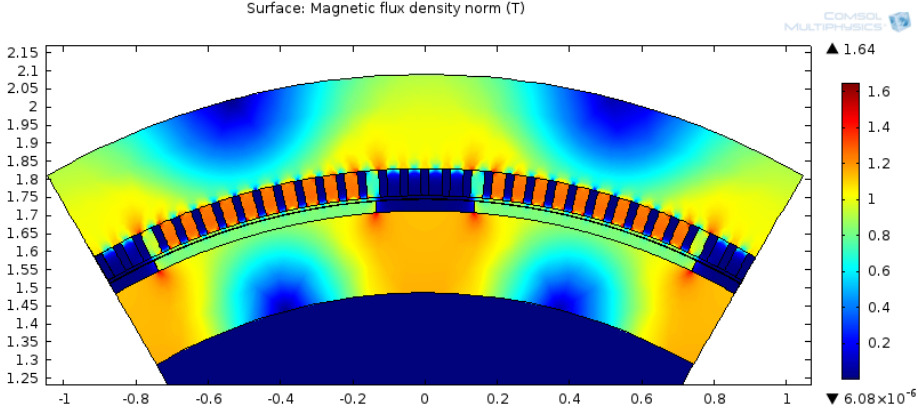


Figure 4.2: Flux density distribution for two poles according to case 1.2.

Figure 4.3 visualizes the flux path in the machine segment. As seen, no flux is going in or escaping radially. In addition, the flux is entering and leaving the mirror axes perpendicularly.

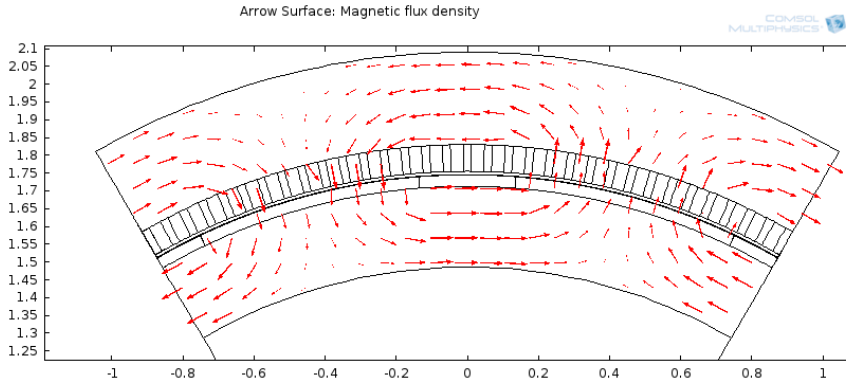


Figure 4.3: Arrow plot to visualize flux path of machine segment including two poles according to case 1.2.

As seen in figure 4.4, the air gap flux density is similar to a square wave shape. This square wave shape was also assumed in the analytical computation. Thus, the shape is not exactly rectangular; the integral of the air gap flux density is the most interesting in the dimensioning of the permanent magnets ideally. The harmonic content in the air gap flux is due to the slotting of the stator. The

frequency and amplitude of these harmonics are relevant to the induced losses, primarily in the permanent magnets.

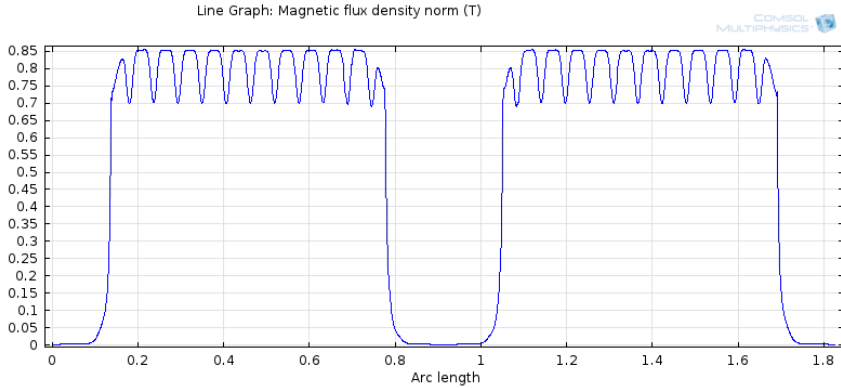


Figure 4.4: Plot of normalized air gap flux close to the magnets according to case 1.2.

4.2.2 Permanent magnet rotor design

In this section, several machines will be evaluated. Firstly, an ordinary machine equipped with field windings will be designed. Next, PM machines will be designed.

- Machine 2.1: Field winding SM
- Machine 2.2: PMSM
- Machine 2.3: PMSM with reduced air gap
- Machine 2.4: PMSM with increased armature loading

The most relevant result parameters are presented in table 4.7. For additional parameters, the complete input and output Excel sheets that were used in the simulations, can be seen in chapter C on page 49.

Although the power factor in the simulations is given at unity, the choice of the power factor has to be regarded in relation to the accepted over-voltage in no-load operation, as described in section 4.1.2. If a lower inductive power factor is chosen, the relative magnetization defined in table 4.7 will be increased.

Machine 2.1 At first, an ordinary SM was constructed by use of the same Matlab code as found in GenProg. Due to the requirement of the high moment of inertia, the machine was relatively short at length, and the diameter large.

Machine 2.2 This machine represents a machine equal to machine 2.1, but the rotor is exchange by a PM rotor.

Machine 2.3 As the synchronous reactance in PMSMs generally is low, the air gap can be reduced to make the magnetization of the machine less demanding. Thus, the amount of permanent material can be reduced.

Machine 2.4 Finally, a more compact machine was computed. In this machine the armature loading was increased, resulting in an increased armature current. Thus, the length of the machine was decreased, making the machine more compact in size. Although, the losses in the armature winding are increased, the total losses are kept approximately constant. In this machine, the rotor ring was increased, to satisfy the requirement of the moment of inertia, thus making the machine heavier.

Table 4.7: Results for the different machines:

Parameter	Symbol	M. 2.1	M. 2.2	M. 2.3	M. 2.4
Apparent power	S_n [MVA]	18	18	18	18
System voltage	V_n [V]	7770	7770	7770	7064
Nominal current	I_n [A]	1338	1338	1338	1471
Power factor	$\cos(\phi)$ [-]	1	1	1	1
Efficiency	η [%]	97.58	97.96	97.96	97.99
Armature loading	A_s [A/cm]	480.3	480.3	480.3	528.4
Inner diameter	D_s [m]	3.51	3.51	3.51	3.51
Gross iron length	l [m]	0.64	0.64	0.64	0.59
Slot height	h_s [mm]	75.1	75.1	75.1	75.1
Height of rotor yoke	h_{yr} [m]	0.272	0.227	0.227	0.500
Minimum air gap	δ [mm]	21	14.7	11.0	13.0
Air gap flux	$\hat{B}_{\delta 1}$ [T]	0.852	0.852	0.852	0.835
Rel. magnetization	E_f/E_{PM} [pu]	1.50	1.09	1.14	1.15
Total losses	P_{tot} [kW]	447	375	375	368
Synch. reactance	x_d [pu]	1.11	0.455	0.596	0.610
Moment of inertia	M [tm ²]	227.6	151.2	150.0	224.8
Machine mass	m [tons]	85.3	63.4	63.2	82.9
Magnet height	h_{PM} [mm]	n/a	47.9	35.3	38.6
Magnet mass	$m_{PM,tot}$ [kg]	n/a	1683	1247	1265

The result of the filtering effect of the stator winding is indicated in figure 4.5. This distribution of the reduction in the harmonic content is calculated by the analytical tool, on the base of the winding factor.

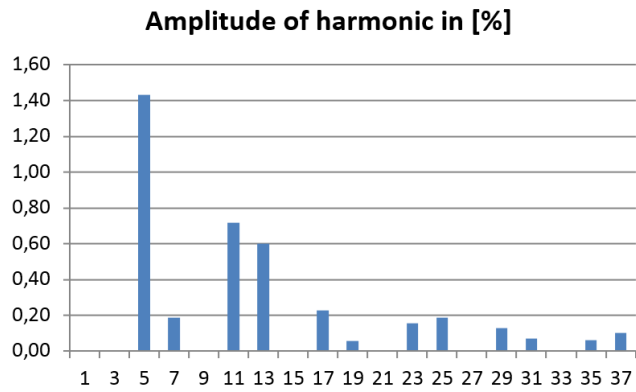


Figure 4.5: Reduced harmonics in percent of the fundamental component.

Chapter 5

Discussion

In this chapter, the simulation results presented in the previous chapter will be discussed, in addition to other relevant elements in this study.

5.1 Validity of the analytical results

The analytical results for different relative pole pitches and air gaps correspond fairly well to the results obtained from the FEM simulation. The different cases simulated had an error from 0.14 % to 6.24 % for the magnet flux density, B_m . For the cases 1.1-1.8, the distinct error of 6.24 % at case 1.5 was clearly greater than the error in the other cases. This may have a coherence to that the relative pole pitch of 0.6 is close to the point of divergence in the iteration of the magnet height. The error tend to increase at decreasing values of α . For values, lower than 0.59, the iteration loop to calculate the magnet height is diverging, thus the Matlab tool is not able to do calculations for such low values of α .

The value of the average air gap flux density, $B_{\delta,av}$, which was intended to be constant in the cases simulated, had an error from 1.57 % to 3.92 %. The other parameters of the machine design were kept constant, where the inner stator diameter $D_s = 3.51 \text{ m}$.

For some variation in the inner stator diameter between 3 and 4 meters, as described in table 4.5, the error is still in the same range as already discussed.

The method to calculate the magnet height described in [11], validates the method by simulations based on a small machine with concentrated windings. The air gap is also significantly smaller in this machine, which is 1 mm. This may affect the accuracy of the results in this study, since the machine simulated are remarkably larger.

An alternative method to assess the validity of the analytical tool could be to perform calculations on a machine with already known specifications, representing a reference machine.

To make calculations in the range of scope in this thesis, the analytical tool is considered sufficiently accurate, where the error is calculated to be below 4 % in

the most relevant cases. Still, the analytical model can be improved to make the results even more exact. The validated range is relatively narrow, as the apparent power of the generator as well as the number of stator slots and the number of poles are kept constant. Further validation is necessary to say if the Matlab tool is valid for computation of other machines.

5.2 The PM rotor design

At first, in this section the numerical values of the results presented for the machines 2.1 to 2.4, will be discussed. Further, some interesting topics in this study will be treated.

The different design alternatives

By exchange of the field winding rotor with a PM rotor, the efficiency was increased from 97.6 to 98.0 %. The machine could may be constructed with even a higher efficiency, if the machine was constructed to be longer, at a smaller diameter. Still, the proposed dimensions express an effective use of the permanent magnet material, although no real optimization of the PM material usage was performed. Further, by additional decrease of the air gap, from 14.7 to 11.0 mm, in machine 2.2 to machine 2.3, the amount of permanent magnet was decreased from 1683 to 1247 kg. In the computation of machine 2.4, the machine was made more compact in size, by a decrease of 5 cm in gross length. In this machine, the air gap was increased from 11.0 to 13.0 mm, to keep the synchronous reactance at approximately 0.6 pu. Due to the increased armature loading, the phase current was rose. Hence, the system voltage appeared at a lower level, to keep the apparent power constant at 18 MVA. In machine 2.4 only a slightly increased demand of PM material is observed, compared to machine 2.3, even if the height of the PM is was increased by 9.4 %, then rise in PM material usage was only 1.4 %. This have to be seen in relation to that the machine was shortened.

Air gap length Compared to an ordinary field winding SM the air gap in a PMSM can be reduced. Due to the high effective air gap including both the physical air gap in addition to the magnet height, the synchronous reactance in the PMSM will be relatively low. A solution to minimize the required magnetization of the machine, is to make the air gap as small as possible. On the other hand, this will result in more distinctive slot harmonics in the air gap flux, and thus increased eddy current losses in the rotor and stator surfaces, especially the permanent magnets.

In this study, no optimization of the air gap length have been calculated, but an air gap resulting in a synchronous reactance about 0.6 pu is assumed suitable. In this way, the air gap is reduced compared to an ordinary field winding SM, but the effects of the armature reaction and the slot harmonics are not affecting the magnet flux density in a too great extent.

Efficiency A design including permanent magnets will occur slightly more efficient compared to the results calculated for a field winding machine. Since no exciting field windings are present, the magnetizing losses can be excluded. On the other hand the permanent magnet can introduce losses in the magnet itself, mainly due to induced eddy currents, but hysteresis losses can also occur at high frequencies [9][10].

Some actions can be implemented to minimize the magnet losses. The eddy current losses can be minimized by introduction of many smaller magnet pieces at each pole, instead of one massive magnet. This will have some of the same effect as the laminations in the stator core. If the segmented magnets are introduced, the relevant equations should include a fill factor, k_{PM} . The introduction of the magnet fill factor will result in a lower effective magnet flux density, and the volume of the permanent magnet have to be increased in a limited extent.

Machine and PM temperature In this thesis, the magnet losses are not one of the objectives. Still, this is of great importance when the machine efficiency is regarded. Magnet power loss will result in heat with a subsequent temperature rise at the rotor and within the permanent magnets. It is important to provide a sufficient cooling of the machine, to keep the temperature within defined limits. This is crucial to the permanent magnet performance via the remanence, when neodymium magnets are employed. Some decrease in the remanence are already accounted for, through the assumption of a relative high operating temperature of the permanent magnet. The results in this thesis do not describe the actual temperature in the machine.

Voltage quality The quality of the induced voltage will be influenced by the shape of the air gap flux density. Ideally, the air gap flux density is of sinusoidal shape, but the design presented will provide a square wave flux density. Due to the constant height of the permanent magnet, the flux density will be fairly constant over the magnet. However, some slot harmonics will be present, as visualized in figure 4.4. Over the magnet spacers the flux density will be approximately zero. If the magnets were modelled with greatest height at the middle, and decreasing height as approaching the ends, the air gap flux density would be smoother and of more sinusoidal shape. This would be similar to the case of field winding machine with its pole head shape described in [2]. Regardless, the armature windings are constructed to filter the air gap flux. Thus, the harmonic content will be depressed efficiently, as described in figure 4.5, where the percentage reduction of each harmonic component is presented based on the winding factor. The reduction of the fifth and the seventh harmonic is remarkable, which is the lowest harmful harmonics [2]. In a symmetrical three phase machine all even and triplen harmonics will not be present.

Moment of inertia A PMSM can be remarkably lighter compared to an ordinary SM at the same power. This reduction in mass will mainly be caused by the alternative rotor construction, since the stator design is kept equal in both cases.

Furthermore, the requirement to the moment of inertia has to be addressed. The moment of inertia has to be according to FIKS [13], in addition to the requirement given by the costumer. The moment of inertia may be lower than required. A lower rotor mass will decrease the value, but in PM rotor construction the equivalent radius of rotation will be larger, as the construction of the poles in a PMSM is more compact compared to an ordinary SM. Which again will affect the moment of inertia at second power, according to equation (2.31) at page 11. If the moment of inertia is calculated to be too low, the height of the rotor yoke can be increased, as in case of machine 2.4. In extreme cases when the moment of inertia is still insufficient, the rotor can be equipped with a flywheel to provide additional moment of inertia.

Transient behavior As described in the results, no values for the transient and sub-transient reactances and time constants are calculated for the PMSM. Ideally, it will not be possible to define a transient or sub-transient period in case of a surface mounted PMSM. These time intervals with the associated parameters are described in [8], for traditional SM in a short circuit situation. When considering the absence of both field windings and damper bars, the PMSM is expected to provide little damping. Still, the permanent magnet itself may provide some damping due to the induced currents in the permanent magnet material.

Alternative design Surface mounted magnets gives the best utilization of the permanent magnet material. Interior magnets waste a significant amount of flux, where approximately 25 % will be leakage flux [2]. On the other hand, embedding will provide better mechanical protection of the magnets. In addition, it may be easier to make a more sinusoidal air gap flux by shaping the pole head instead of shaping the magnet. A machine at the power rating presented should also be equipped with damper bars according to FIKS [13]. A design including damper bars may be easier and more suitable in an interior magnet machine, since the damper bars can be placed in the pole head.

Chapter 6

Conclusion

In this study, an analytical Matlab program has been modified to make computations for PMSMs, in addition to its original capability of field winding SM computation. The theoretical background, including the relevant equations is presented in this thesis. When developing the Matlab script the main focus has been on the rotor, therefore parts of the script, for example the dimensioning of the stator will be equal for both types of machines.

The analytical design tool has been verified by FEM analysis in COMSOL. Simulations in no-load operation were executed through ten different cases, where air gap, magnet width, and diameter of the machine were varied. The other input parameters were kept constant. When comparing the results an error was expressed. This was below 4 % in the most relevant cases, regarding both the magnet and air gap average flux densities. Hence, the accuracy of the analytical model is found sufficient in this study, but additional verification may be required considering other machines.

In the proposal of the PMSM design, simulations were performed on four different machines. The series of simulations were initiated on design of a field winding machine, by following PM redesign of this machine. Most of the input parameters were kept constant, but some variation in air gap length, rotor yoke height and armature loading occurred. It was observed that the field winding machine could be redesigned by PM magnetization, and increase the efficiency from 97.6 to 98.0 % of the 18 MVA machine. The losses in the PM itself were neglected.

By comparison of the machines, the physical air gap in the PMSM can be reduced, due to the high magnetic air gap. Machine 2.1 had an air gap at 21.0 mm, while machine 2.3 had an air gap equal to 11.0 mm, after reduction. In regard of the synchronous reactance, this will be low in PMSM. After the air gap was reduced in machine 2.3 and 2.4, the synchronous reactance was calculated to be approximately 0.6 pu in both machines, in contrast to x_d equal to 1.1 pu in machine 2.1.

Due to the alternative rotor construction with PM, the rotor can be constructed remarkably lighter. The machine mass can be reduced from 85 to 63

tons. The reduction in rotor mass do also affect the moment of inertia, which will be reduced in machine 2.2 and 2.3, from 228 to approximately 150 tm^2 . If a high moment of inertia is needed, the height of the rotor yoke can be increased, as for machine 2.4. Then the moment of inertia equals the value of machine 2.1.

The amount of PM material needed is calculated to be 1683 kg in machine 2.2, at a magnet height equal to 47.9 mm. The material demand is reduced to 1247 kg in machine 2.3 at a magnet height of 35.3 mm, after reduction of the air gap. At last, in machine 2.4, the armature loading was increased from 480 to 528 A/cm . This resulted in a shortening of 5 cm in iron gross length, to a length of 0.59 m. Compared to machine 2.3, only a slight increase in PM mass of 1.4 % was observed, while the increase in magnet height was of 9.4 %. The efficiency in this machine was equal to the other PMSMs, at 98.0 %.

Chapter 7

Recommendations for further work

The following tasks are suggestions for further work:

- Verify the analytical Matlab tool for a wider range of PMSM.
- Include calculation of the losses in the permanent magnets.
- Depending of the previous item, the heat flow can be calculated for the PMSM, including temperatures for the different parts of the machine.
- Make the computation more efficient. The current solution has an issue with reading from and writing to the Excel files, this is consuming the most of the time when running the script.

Bibliography

- [1] S. C. Wedum *PM synchronous machine for pumped storage hydro plant*. Specialization project, NTNU, Trondheim, Norway, 2014
- [2] J. Pyrhönen, T. Jokinen, V. Hrabovcová, *Design of rotating electrical machines*. John Wiley & Sons, Ltd., Chichester U.K., 2008.
- [3] D. C. Hanselman, *Brushless permanent-magnet motor design*. McGraw-Hill, New York, U.S., 1994.
- [4] TDK, *NEOREC series: Neodymium-Iron-Boron Magnets*, May 2011. [cited 2015 May 11] Available from: <http://product.tdk.com/en/catalog/datasheets/e331.pdf>.
- [5] I. Vikan, A. Lundseng, *Beregning av vannkraftgeneratorer*. NTNU, Department of Electric power engineering, Trondheim, Norway, 2009.
- [6] I. Vikan, A. Lundseng, *Generator design for hydropower station upgrade*. NTNU, Department of Electric power engineering, Trondheim, Norway, 2010.
- [7] E. Westgaard, O. W. Andersen, *Dimensjoneringseksempel for synkronmaskin*. NTH, Department of Electrical machines, Trondheim Norway, 1965.
- [8] J. Machowski, J. W. Bialek, J. R. Bumby, *Power system stability and control*. John Wiley & Sons, Ltd., Chichester U.K., 2nd Edition, 2008.
- [9] D. Ishak, Z. Q. Zhu, D. Howe, *Eddy-current loss in the rotor magnets of permanent-magnet brushless machines having a fractional number of slots per pole* IEEE Transactions on magnetics, Vol. 41, NO. 9, September 2005.
- [10] A. Fukuma, S. Kanazawa, D. Miyagi, N. Takahashi, *Investigation of SC loss of permanent magnet of SPM motor considering hysteresis and eddy-current losses* IEEE Transactions on magnetics, Vol. 41, NO. 5, May 2005.
- [11] R. Qu, T. A. Lipo, *Analysis and modelling of air-gap and zigzag leakage fluxes in surface mounted permanent-magnet machine* IEEE Transactions on industry applications, Vol. 40, NO. 1, January/February 2004.
- [12] R. K. Nilssen, *Electromagnetics in power engineering*. NTNU, Department of Electric power engineering, Trondheim Norway, 2010.

BIBLIOGRAPHY

- [13] Statnett, *FIKS - Funksjonskrav i kraftsystemet*. Oslo, Norway, 2012.

Appendix A

Initialization of GenProg

This is primarily a rendering of material described in [6]. To make it easier to understand how to use the GenProg programs, the technique will be described briefly in this section. The relevant equations, which make the base of the PM specific part of the program, are described in section 2. The general part of the program including the equations is described in [6].

Initially the relevant program files have to be placed in the desired folder:

- GenProg2.m
- Input.xls
- Output.xls
- sporfil.xls
- Int.m

The files sporfil.xls and Output.xls have to be closed prior the computation process. If the files are remained open, Matlab will not be able to write to these files.

In general, the computation process is divided into three parts:

- Input
- Computation/simulation
- Output

Where both reading input and writing output are time-consuming processes.

Input All values in the *Required Values* in *Input.xls* have to be defined, to make the program able to perform the calculations. If the moment of inertia, M is not known, it can be set to zero. Then the program will calculate a suitable value of this parameter.

Computation When the current folder are defined to be the folder including all the necessary files, the simulation can be started. By typing *GenProg2* in the command window in Matlab, the program will run. When the design of a

new machine is present, the following values have to be chosen in the command window:

- Number of slots (can be chosen from *sporfil.xls*)
- Number of parallel circuits
- Number of turns per coil
- Coil pitch

If these values are satisfying, they should be written into the table *Optional Values* in *Input.xls* prior the next simulation. This will save some time, since the values do not have to be redefined in every simulation. The progress of the program can be followed in the command window.

Output The computed values will be written into the file *Output.xls*. Out of these values several supplementing values can be defined prior the next simulation.

To optimize the design, it may be necessary to repeat the computation process several times.

Appendix B

Relevant tables

Table B.1: Characteristics of neodymium and samarium cobalt magnets [2][4]:

	Neodymium magnets	SmCo magnets
Composition	Nd, Fe, B, etc.	Sm, Co, Fe, Cu, etc.
Production	Sintering	Sintering
Energy product	199–310 kJ/m ³	255 kJ/m ³
Remanence	1.03–1.3 T	0.82–1.16 T
Intrinsic coercive force, H_{cJ}	875 kA/m to 1.99 MA/m	493 kA/m to 1.59 MA/m
Relative permeability	1.05	1.05
Reversible temperature coefficient of remanence	–0.11 to –0.13%/K	–0.03 to –0.04%/K
Reversible temperature coefficient of coercive H_{cJ}	–0.55 to –0.65%/K	–0.15 to –0.30%/K
Curie temperature	320 °C	800 °C
Density	7300–7500 kg/m ³	8200–8400 kg/m ³
Coefficient of thermal expansion in magnetizing direction	$5.2 \times 10^{-6}/K$	$5.2 \times 10^{-6}/K$
Coefficient of thermal expansion normal to magnetizing direction	$-0.8 \times 10^{-6}/K$	$11 \times 10^{-6}/K$
Bending strength	250 N/mm ²	150 N/mm ²
Compression strength	1100 N/mm ²	800 N/mm ²
Tensile strength	75 N/mm ²	35 N/mm ²
Vickers hardness	550–650	500–550
Resistivity	$110\text{--}170 \times 10^{-8} \Omega \text{ m}$	$86 \times 10^{-8} \Omega \text{ m}$
Conductivity	590 000–900 000 S/m	1160 000 S/m

APPENDIX B. RELEVANT TABLES

Table B.3: Permeance factors of the end windings in a synchronous machine [2]:







Cross-section of end winding	Nonsalient-pole machine		Salient-pole machine	
	λ_{lew}	λ_w	λ_{lew}	λ_w
	0.342	0.413	0.297	0.232
	0.380	0.130	0.324	0.215
	0.371	0.166	0.324	0.243
	0.493	0.074	0.440	0.170
	0.571	0.073	0.477	0.187
	0.605	0.028	0.518	0.138

Table B.4: Coefficient γ for definition of the air gap [2]:

Salient-pole constant air-gap synchronous machines	$\gamma = 7.0 \times 10^{-7}$
Salient-pole synchronous machines, the air gap of which is shaped to produce a sinusoidal flux density distribution	$\gamma = 4.0 \times 10^{-7}$
Nonsalient-pole synchronous machines	$\gamma = 3.0 \times 10^{-7}$
DC machines without compensating winding	$\gamma = 3.6 \times 10^{-7}$
DC machines without compensating winding and commutating poles	$\gamma = 5.0 \times 10^{-7}$
Compensated DC machines	$\gamma = 2.2 \times 10^{-7}$

Table B.2: Slot alternatives:

Q	q	fullpitch	coil span	pitch fraction
90	2,500	7,5	6	0,800
96	2,667	8	7	0,875
102	2,833	8,5	7	0,824
108	3,000	9	7	0,778
114	3,167	9,5	8	0,842
120	3,333	10	8	0,800
126	3,500	10,5	9	0,857
132	3,667	11	9	0,818
138	3,833	11,5	10	0,870
144	4,000	12	10	0,833
150	4,167	12,5	10	0,800
156	4,333	13	11	0,846
162	4,500	13,5	11	0,815
168	4,667	14	12	0,857
174	4,833	14,5	12	0,828
180	5,000	15	12	0,800
186	5,167	15,5	13	0,839
192	5,333	16	13	0,813
198	5,500	16,5	14	0,848
204	5,667	17	14	0,824
210	5,833	17,5	15	0,857
216	6,000	18	15	0,833
222	6,167	18,5	15	0,811
228	6,333	19	16	0,842
234	6,500	19,5	16	0,821
240	6,667	20	17	0,850
246	6,833	20,5	17	0,829
252	7,000	21	17	0,810
258	7,167	21,5	18	0,837
264	7,333	22	18	0,818
270	7,500	22,5	19	0,844
276	7,667	23	19	0,826
282	7,833	23,5	19	0,809
288	8,000	24	20	0,833
294	8,167	24,5	20	0,816

Appendix C

Input and output for the rotor design

C.1 Input machine 2.1

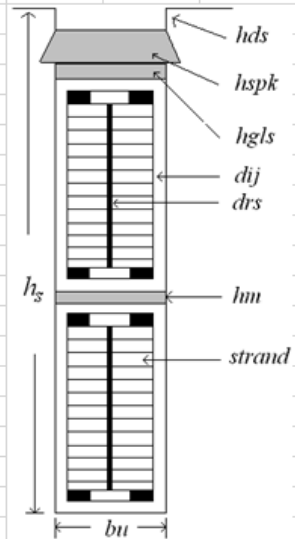
Generator specifications			
Required values:			
Apparent power	Sn	18 MVA	
Power factor	Cosphi	1	
Frequency	f	50 Hz	
Number of poles	Np	12 poles	
Runaway speed	nr	850 rpm	
Maximum temperatur rise	dTmx	60	
Moment of inertia	M	56,25 tm ²	
Generator maximum voltage	Vmx	15 kV	
Maximum value of synchronous reactance	xd	1,1 pu	
Maximum value of transient reactance	xd1	0,4 pu	
Minimum value of subtransient reactance	xd2	0,15 pu	
Maximum tooth flux density	Btmx	1,8 T	
Maximum pole core flux density	Bpmx	1,6 T	
Maximum yoke flux density	Bymx	1,2 T	
Specify ratio	bsdbt	0,6	
Core section length	bcs	0,04 m	
Cooling duct length	bv	0,006 m	
Filling factor (iron core)	kFe	0,95	
Current density in stator winding	Ss	3,5 A/mm ²	
Height of one strand i the statorbar	hcus	2,2 mm	
Required feild voltage	Vf	125 V	
Current density in rotor winding	Sf	3 A/mm ²	
Negative sequence voltage	Vnmx	20 %	
Skewving (in number of slots)	s	0 spor	
Outer diameter of shaft	Dri	0,3 m	
Relative pole pitch	alfa	0,7	
Remanent flux density	Br	0 T	
Relative permeability of PM	myr	0	
Optional Values:			
Do calculations for PM machine	Pmcalc	0 1=YES	0=Default
Nominal Voltage	Un	0 V	0=Default
Utilization factor	C	5	0=Default
Number of Slots	Qs	198	0=Default
Number of Parallel Circuits	pnr	1	0=Default
Number of Turns per Coil	tnr	1	0=Default
Coil Span	y	14 slots	0=Default

C.1. INPUT MACHINE 2.1

Inner Diameter of Stator	Di	3,51 m	0=Default
Gross Iron Length	lb	0 m	0=Default
Air Gap Flux Density	B δ	0 T	0=Default
Height of rotor yoke	hyr	0 m	0=Default
Cooling Air Flow	qth	0 m ³ /s	0=Default
Flywheel	GD2add	0 kg	0=Default
Minimum air gap	delta0	21 mm	0=Default
Field Winding Width	bctf	0 m	0=Default
Specific Iron Loss, at 1 Tesla	P10	0 W/kg	0=Default
Use old iron sheets (1950-1960)	FeOld	0 1=YES	0=Default
Average Stator Coil Length	lav	0 m	0=Default
Slot Dimensions			
Slot Height	hs	0 m	0=Default
Slot Width	bu	0 m	
Number of strands in a Bar	ndl	0	
Number of Strands per Turn	ndlp	0	
Nr. of Strand on Top of each other per Turn	ndlh	0	
Total Copper Width in Slot	bcus	0 m	
Distance from Slot Wedge to Air Gap	hds	0 m	
Slot Wedge Thickness	hspk	0 m	
Slot Wedge Spacer (glidestrimmel)	hgls	0 m	
Bar Separator (mellomstrimmel)	hm	0 m	
Roebel Separator	drs	0 m	
Earth Insulation Thickness	dij	0 m	
Strand Insulation Thickness	dicu	0 m	
Winding Insulation Thickness	diw	0 m	
Pole Dimensions			
Pole Shoe Width	bps	0 m	0=Default
Pole Shoe Height	hps	0 m	0=Default
Pole Core Width	bpk	0 m	0=Default
Pole Core Height	hpk	0 m	0=Default
Total Field Winding Height	hf	0 m	0=Default
Number of turns in Field Winding	nf	0	0=Default
Height of a Field Winding	hcuf	0 m	0=Default
Number of Damper Bars	NDs	0 m	0=Default
Magnetizing Losses	Pmagn	0 kW	0=Default
Insulation between winding and pole core	bi	0 m	0=Default
Field winding insulation	bif	0 m	0=Default

C.2 Output machine 2.1

Main Data			
Apparent Power	Sn	18	MVA
System Voltage	Un	7769,8	V
Nominal Current	In	1337,5	A
Cosphi		1	
Efficiency	η	97,575	%
Rotational Speed	ns	500	rpm
Stator Parameters			
Utilization Factor	C	5,00	
Armature Loading	As	480,33	A/cm
Inner Diameter	Di	3,51	m
Outer Diameter	Dy	4,18	m
Gross Iron Length	lb	0,64	m
Net Iron Length	ln	0,56	m
Number of Slots	Qs	198,00	slots
Number of Cooling Ducts	nv	13,00	
Number of Turns Per Phase	Ns	66,00	
Number of Turns per Coil	tnr	1,00	
Number of Parallel Circuits	pnr	1,00	
Slots per pole and phase	q	5,50	
Relative polepitch	y	0,85	
Coil Span	Ww	14,00	slots
Winding Factor	kw	0,93	
Sloth Hight	hs	75,10	mm
Sloth width	bu	20,88	mm
Tooth width	bd	34,81	mm
Slot Pitch	tu	55,69	mm
Number of strands per bar	ndl	22,00	
Height of a Strand	hcus	2,20	mm
Width of a Strand	bcus	7,87	mm
Main Insulation	dij	2,13	mm
Strand Insulation	dicu	0,10	mm
Winding lenght	lav	3,96	m
Cross Section of Stator Bar	Acus	373,12	mm ²
Stator Current Density	Ss	3,58	A/mm ²
Stator Winding Resistance	Rdc20	0,01	Ω
Stator Winding Resistance	Rdc75	0,02	Ω
			Per Phase Resistance (20 °C)
			Per Phase Resistance (75 °C)



C.2. OUTPUT MACHINE 2.1

Stator Wdg. Resistance Factor	Kra	1,02				
Slot Resistance Factor	Krad	1,06				
Maximum Resistance Factor	Kmax	1,19			<i>For the topmost strand</i>	
Skewing	s	0,00	slots			

Rotor Parameters

Minimum Air Gap	δ_0	21,0	mm			
Equivalent average Air Gap	δ_m	26,2	mm			
Pole Shoe width	bps	635,9	mm			
Pole Shoe Height	hps	50,0	mm			
Pole Core Width	bpc	464,9	mm			
Pole Core Height	hpc	121,4	mm			
Number of Turns per Pole	nf	65,0				
Field Current	If	347,8	A			
Field Winding Width	bcuf	86,9	mm			
Field Winding Height	hcuf	1,4	mm			
Cross Section of Field Winding	Af	117,6	mm ²			
Current Density, Field Winding	Sf	3,0	A/mm ²			
Rotor Winding Resistance	Rf20	0,3	Ω		<i>Field Wind. Resistance (20 °C)</i>	
Rotor Winding Resistance	Rf75	0,4	Ω		<i>Field Wind. Resistance (75 °C)</i>	
Relative Pole Width	α	0,70				
Number of Damperbars	NDs	10,0				
Cross Section of Damper Bar	AcuD	171,6	mm ²			
Clearance, Pole Windings	polklaring	187,7	mm			

Magnetic Parameters

Air Gap	0,852	T	15206	At	<i>(peak of fundamental)</i>
Stator Core	1,200	T	103	At	
Stator Tooth	1,635	T	236	At	
Rotor Ring	1,118	T	31	At	
Pole Core/Inside PM	1,243	T	165	At	<i>(max at bottom of core)</i>
Relative Magnetization	Ef		1,449	pu	
Relative Induced Voltage	Ei		1,009	pu	
Total Required Magnetization	Θ_{mn}		22609	At	
Leakage flux	FIL		11,27	%	

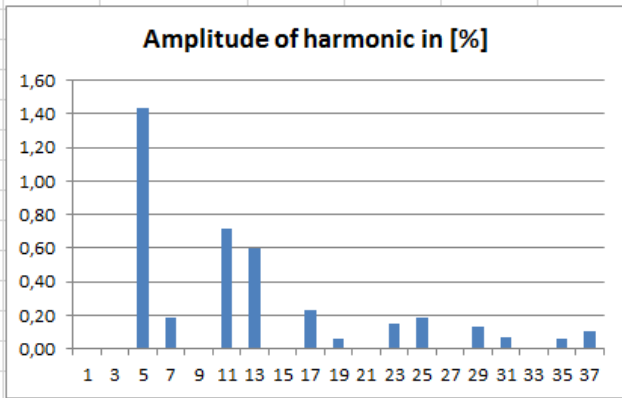
APPENDIX C. INPUT AND OUTPUT FOR THE ROTOR DESIGN

Loss Calculations				
No load:				
Iron Loss Stator Core	Pfe	44,2	kW	
Windage and Bearing Loss	Pfw	212,8	kW	
Kopper Loss Rotor (No-load)	Prl	31,2	kW	
Full load:				
DC- stator loss	Pcusdc	86,2	kW	
AC-stator	Pcusac	1,7	kW	
Additional Kopper Loss Rotor	Prfl	14,0	kW	
Additional loss	Padd	54,1	kW	
Magnetizing losses	Pmagn	3,2	kW	
Total Losses	Ptot	447,3	kW	
Reactances and Time Constants				
Armature Reaction Reactance	Xmd	1,013	pu	
	Xmq	0,570	pu	
Leakage Reactance	Xσ	0,094	pu	
	Xd	1,107	pu	
Synchronous Reactance	Xq	0,664	pu	
	X'd	0,202	pu	
Transient Reactance	X''d	0,158	pu	
	X''q	0,182	pu	
Transient Time Constant	T'd	0,581	s	
Sub-Transient Time Constant	T''d	0,020	s	
	T''q	0,016	s	
Thermal Calculations				
Cooling Air Flow	qth	6,8	m ³ /s	
Maximal Air Speed	vim	12,7	m/s	
Mechanical Calculations				
Calculated Moment of Inertia	M	56,9	tm ²	
Weight of Machine	m	85,3	tons	
Maximum peripheral velocity	Vr	156,22	m/s	

C.2. OUTPUT MACHINE 2.1

Harmonic components in the machine

Harm.Nr.	Amplitude
1	0,00
3	0,00
5	1,43
7	0,19
9	0,00
11	0,72
13	0,60
15	0,00
17	0,23
19	0,06
21	0,00
23	0,15
25	0,19
27	0,00
29	0,13
31	0,07
33	0,00
35	0,06
37	0,10



Telephone Harmonic Factor THF 0,005578 %

PM machine results

Remanent flux density	Br	0 T
Relative permeability of PM	myr_pm	0
Dimensions of PM		
Height	hpm	0,00 mm
Surface area of each PM	Am	0,0000 m ²
Cross-section area of each PM	Am_cross	0,0000 m ²
Volume of each PM	V_pm	0,0000 m ³
Totalt mass	m_pm_tot	0,00 kg

C.3 Input machine 2.2

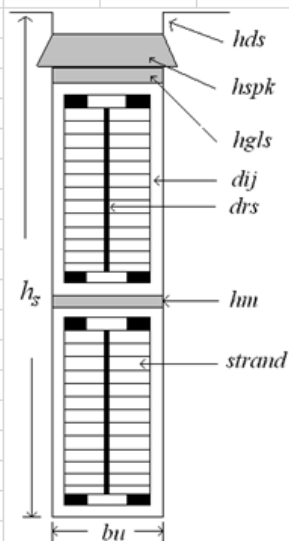
Generator specifications				
Required values:				
Apparent power	Sn	18	MVA	
Power factor	Cosphi	1		
Frequency	f	50	Hz	
Number of poles	Np	12	poles	
Runaway speed	nr	850	rpm	
Maximum temperatur rise	dTmx	60		
Moment of inertia	M	56,25	tm ²	
Generator maximum voltage	Vmx	15	kV	
Maximum value of synchronous reactance	xd	1,1	pu	
Maximum value of transient reactance	xd1	0,4	pu	
Minimum value of subtransient reactance	xd2	0,15	pu	
Maximum tooth flux density	Btmx	1,8	T	
Maximum pole core flux density	Bpmx	1,6	T	
Maximum yoke flux density	Bymx	1,2	T	
Specify ratio	bsdbt	0,6		
Core section length	bcs	0,04	m	
Cooling duct length	bv	0,006	m	
Filling factor (iron core)	kFe	0,95		
Current density in stator winding	Ss	3,5	A/mm ²	
Height of one strand i the statorbar	hcus	2,2	mm	
Required feild voltage	Vf	125	V	
Current density in rotor winding	Sf	3	A/mm ²	
Negative sequence voltage	Vnmx	20	%	
Skewing (in number of slots)	s	0	spor	
Outer diameter of shaft	Dri	0,3	m	
Relative pole pitch	alfa	0,7		
Remanent flux density	Br	1,14	T	
Relative permeability of PM	myr	1,05		
Optional Values:				
Do calculations for PM machine	Pmcalc	1	1=YES	0=Default
Nominal Voltage	Un	0	V	0=Default
Utilization factor	C	5		0=Default
Number of Slots	Qs	198		0=Default
Number of Parallel Circuits	pnr	1		0=Default
Number of Turns per Coil	tnr	1		0=Default
Coil Span	y	14	slots	0=Default

C.3. INPUT MACHINE 2.2

Inner Diameter of Stator	Di	3,51	m	0=Default
Gross Iron Length	lb	0	m	0=Default
Air Gap Flux Density	B δ	0	T	0=Default
Height of rotor yoke	hyr	0	m	0=Default
Cooling Air Flow	qth	0	m ³ /s	0=Default
Flywheel	GD2add	0	kg	0=Default
Minimum air gap	delta0	0	mm	0=Default
Field Winding Width	bcuf	0	m	0=Default
Specific Iron Loss, at 1 Tesla	P10	0	W/kg	0=Default
Use old iron sheets (1950-1960)	FeOld	0	1=YES	0=Default
Average Stator Coil Length	lav	0	m	0=Default
Slot Dimensions				
Slot Height	hs	0	m	0=Default
Slot Width	bu	0	m	
Number of strands in a Bar	ndl	0		
Number of Strands per Turn	ndlp	0		
Nr. of Strand on Top of each other per Turn	ndlh	0		
Total Copper Width in Slot	bcus	0	m	
Distance from Slot Wedge to Air Gap	hds	0	m	
Slot Wedge Thickness	hspk	0	m	
Slot Wedge Spacer (glidestrimmel)	hgls	0	m	
Bar Separator (mellonstrimmel)	hm	0	m	
Roebel Separator	drs	0	m	
Earth Insulation Thickness	dij	0	m	
Strand Insulation Thickness	dicu	0	m	
Winding Insulation Thickness	diw	0	m	
Pole Dimensions				
Pole Shoe Width	bps	0	m	0=Default
Pole Shoe Height	hps	0	m	0=Default
Pole Core Width	bpk	0	m	0=Default
Pole Core Height	hpk	0	m	0=Default
Total Field Winding Height	hf	0	m	0=Default
Number of turns in Field Winding	nf	0		0=Default
Height of a Field Winding	hcuf	0	m	0=Default
Number of Damper Bars	NDS	0	m	0=Default
Magnetizing Losses	Pmagn	0	kW	0=Default
Insulation between winding and pole core	bi	0	m	0=Default
Field winding insulation	bif	0	m	0=Default

C.4 Output machine 2.2

Main Data			
Apparent Power	Sn	18	MVA
System Voltage	Un	7769,8	V
Nominal Current	In	1337,5	A
Cosphi		1	
Efficiency	η	97,960	%
Rotational Speed	ns	500	rpm
Stator Parameters			
Utilization Factor	C	5,00	
Armature Loading	As	480,33	A/cm
Inner Diameter	Di	3,51	m
Outer Diameter	Dy	4,18	m
Gross Iron Length	lb	0,64	m
Net Iron Length	ln	0,56	m
Number of Slots	Qs	198,00	slots
Number of Cooling Ducts	nv	13,00	
Number of Turns Per Phase	Ns	66,00	
Number of Turns per Coil	tnr	1,00	
Number of Parallel Circuits	pnr	1,00	
Slots per pole and phase	q	5,50	
Relative polepitch	y	0,85	
Coil Span	Ww	14,00	slots
Winding Factor	kw	0,93	
Sloth Hight	hs	75,10	mm
Sloth width	bu	20,88	mm
Tooth width	bd	34,81	mm
Slot Pitch	ru	55,69	mm
Number of strands per bar	ndl	22,00	
Height of a Strand	hcus	2,20	mm
Width of a Strand	bcus	7,87	mm
Main Insulation	dij	2,13	mm
Strand Insulation	dicu	0,10	mm
Winding lenght	lav	3,96	m
Cross Section of Stator Bar	Acus	373,12	mm ²
Stator Current Density	Ss	3,58	A/mm ²
Stator Winding Resistance	Rdc20	0,01	Ω Per Phase Resistance (20 °C)
Stator Winding Resistance	Rdc75	0,02	Ω Per Phase Resistance (75 °C)



C.4. OUTPUT MACHINE 2.2

Stator Wdg. Resistance Factor	Kra		1,02				
Slot Resistance Factor	Krad		1,06				
Maximum Resistance Factor	Kmax		1,19			<i>For the topmost strand</i>	
Skewing	s		0,00	slots			
Rotor Parameters							
Minimum Air Gap	δ_0		14,7	mm			
Equivalent average Air Gap	δ_m		15,1	mm			
Pole Shoe width	bps		0,0	mm			
Pole Shoe Height	hps		0,0	mm			
Pole Core Width	bpc		0,0	mm			
Pole Core Height	hpc		0,0	mm			
Number of Turns per Pole	nf		0,0				
Field Current	If		0,0	A			
Field Winding Width	bcuf		0,0	mm			
Field Winding Height	hcuf		0,0	mm			
Cross Section of Field Winding	Af		0,0	mm ²			
Current Density, Field Winding	Sf		0,0	A/mm ²			
Rotor Winding Resistance	Rf20		0,0	Ω		<i>Field Wind. Resistance (20 °C)</i>	
Rotor Winding Resistance	Rf75		0,0	Ω		<i>Field Wind. Resistance (75 °C)</i>	
Relative Pole Width	α		0,70				
Number of Damperbars	NDs		0,0				
Cross Section of Damper Bar	AcuD		0,0	mm ²			
Clearance, Pole Windings	polklaring		0,0	mm			
Magnetic Parameters							
Air Gap	0,852	T	0	At		<i>(peak of fundamental)</i>	
Stator Core	1,211	T	0	At			
Stator Tooth	1,633	T	0	At			
Rotor Ring	1,229	T	0	At			
Pole Core/Inside PM	0,816	T	0	At		<i>(max at bottom of core)</i>	
Relative Magnetization	Ef		1,086	pu			
Relative Induced Voltage	Ei		1,009	pu			
Total Required Magnetization	Θ_{mn}		0	At			
Leakage flux	FIL		1,51	%			

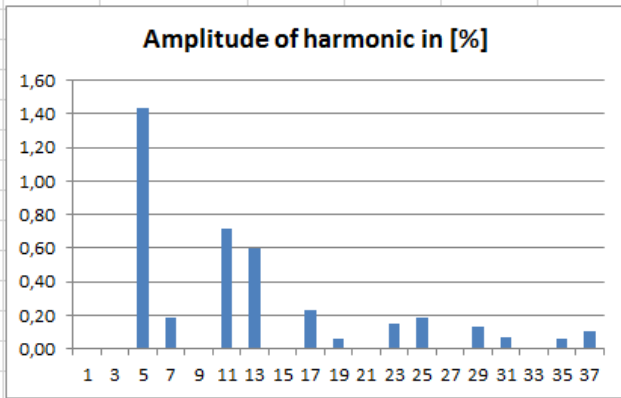
APPENDIX C. INPUT AND OUTPUT FOR THE ROTOR DESIGN

Loss Calculations				
No load:				
Iron Loss Stator Core	Pfe	44,6	kW	
Windage and Bearing Loss	Pfw	212,8	kW	
Kopper Loss Rotor (No-load)	Prl	0,0	kW	
Full load:				
DC- stator loss	Pcusdc	86,2	kW	
AC-stator	Pcusac	1,7	kW	
Additional Kopper Loss Rotor	Prfl	0,0	kW	
Additional loss	Padd	29,5	kW	
Magnetizing losses	Pmagn	0,0	kW	
Total Losses	Ptot	374,9	kW	
Reactances and Time Constants				
Armature Reaction Reactance	Xmd	0,366	pu	
	Xmq	0,000	pu	
Leakage Reactance	Xσ	0,089	pu	
	Xd	0,455	pu	
Synchronous Reactance	Xq	0,000	pu	
	X'd	0,000	pu	
Sub-Transient Reactance	X''d	0,000	pu	
	X''q	0,000	pu	
Transient Time Constant	T'd	0,000	s	
Sub-Transient Time Constant	T''d	0,000	s	
	T''q	0,000	s	
Thermal Calculations				
Cooling Air Flow	qth	4,8	m ³ /s	
Maximal Air Speed	vim	8,9	m/s	
Mechanical Calculations				
Calculated Moment of Inertia	M	37,8	tm ²	
Weight of Machine	m	63,4	tons	
Maximum peripheral velocity	Vr	156,22	m/s	

C.4. OUTPUT MACHINE 2.2

Harmonic components in the machine

Harm.Nr.	Amplitude				
1	0,00				
3	0,00				
5	1,43				
7	0,19				
9	0,00				
11	0,72				
13	0,60				
15	0,00				
17	0,23				
19	0,06				
21	0,00				
23	0,15				
25	0,19				
27	0,00				
29	0,13				
31	0,07	Telephone Harmonic Factor	THF	0,005578 %	
33	0,00				
35	0,06				
37	0,10				



PM machine results

Remanent flux density	Br	1,14 T		
Relative permeability of PM	myr_pm	1,05		
Dimensions of PM				
Height	hpm	47,86 mm		
Surface area of each PM	Am	0,4104 m ²		
Cross-section area of each PM	Am_cross	0,0301 m ²		
Volume of each PM	V_pm	0,0192 m ³		
Totalt mass	m_pm_tot	1682,64 kg		

C.5 Input machine 2.3

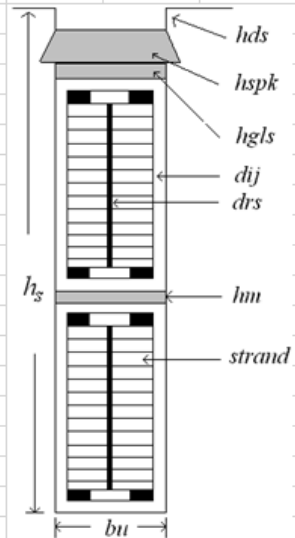
Required values:				
Apparent power	Sn	18	MVA	
Power factor	Cosphi	1		
Frequency	f	50	Hz	
Number of poles	Np	12	poles	
Runaway speed	nr	850	rpm	
Maximum temperatur rise	dTmx	60		
Moment of inertia	M	56,25	tm ²	
Generator maximum voltage	Vmx	15	kV	
Maximum value of synchronous reactance	xd	1,1	pu	
Maximum value of transient reactance	xd1	0,4	pu	
Minimum value of subtransient reactance	xd2	0,15	pu	
Maximum tooth flux density	Btmx	1,8	T	
Maximum pole core flux density	Bpmx	1,6	T	
Maximum yoke flux density	Bymx	1,2	T	
Specify ratio	bsdbt	0,6		
Core section length	bcs	0,04	m	
Cooling duct length	bv	0,006	m	
Filling factor (iron core)	kFe	0,95		
Current density in stator winding	Ss	3,5	A/mm ²	
Height of one strand i the statorbar	hcus	2,2	mm	
Required feild voltage	Vf	125	V	
Current density in rotor winding	Sf	3	A/mm ²	
Negative sequence voltage	Vnmx	20	%	
Skewving (in number of slots)	s	0	spor	
Outer diameter of shaft	Dri	0,3	m	
Relative pole pitch	alfa	0,7		
Remanent flux density	Br	1,14	T	
Relative permeability of PM	myr	1,05		
Optional Values:				
Do calculations for PM machine	Pmcalc	1	1=YES	0=Default
Nominal Voltage	Un	0	V	0=Default
Utilization factor	C	5		0=Default
Number of Slots	Qs	198		0=Default
Number of Parallel Circuits	pnr	1		0=Default
Number of Turns per Coil	tnr	1		0=Default
Coil Span	y	14	slots	0=Default

C.5. INPUT MACHINE 2.3

Inner Diameter of Stator	Di	3,51 m	0=Default
Gross Iron Length	lb	0 m	0=Default
Air Gap Flux Density	B δ	0 T	0=Default
Height of rotor yoke	hyr	0 m	0=Default
Cooling Air Flow	qth	0 m ³ /s	0=Default
Flywheel	GD2add	0 kg	0=Default
Minimum air gap	delta0	11 mm	0=Default
Field Winding Width	bcuf	0 m	0=Default
Specific Iron Loss, at 1 Tesla	P10	0 W/kg	0=Default
Use old iron sheets (1950-1960)	FeOld	0 1=YES	0=Default
Average Stator Coil Length	lav	0 m	0=Default
Slot Dimensions			
Slot Height	hs	0 m	0=Default
Slot Width	bu	0 m	
Number of strands in a Bar	ndl	0	
Number of Strands per Turn	ndlp	0	
Nr. of Strand on Top of each other per Turn	ndlh	0	
Total Copper Width in Slot	bcus	0 m	
Distance from Slot Wedge to Air Gap	hds	0 m	
Slot Wedge Thickness	hspk	0 m	
Slot Wedge Spacer (glidestrimmel)	hgl	0 m	
Bar Separator (mellonstrimmel)	hm	0 m	
Roebel Separator	drs	0 m	
Earth Insulation Thickness	dij	0 m	
Strand Insulation Thickness	dicu	0 m	
Winding Insulation Thickness	diw	0 m	
Pole Dimensions			
Pole Shoe Width	bps	0 m	0=Default
Pole Shoe Height	hps	0 m	0=Default
Pole Core Width	bpc	0 m	0=Default
Pole Core Height	hpc	0 m	0=Default
Total Field Winding Height	hf	0 m	0=Default
Number of turns in Field Winding	nf	0	0=Default
Height of a Field Winding	hcuf	0 m	0=Default
Number of Damper Bars	Nds	0 m	0=Default
Magnetizing Losses	Pmagn	0 kW	0=Default
Insulation between winding and pole core	bi	0 m	0=Default
Field winding insulation	bif	0 m	0=Default

C.6 Output machine 2.3

Main Data			
Apparent Power	Sn	18 MVA	
System Voltage	Un	7769,8 V	
Nominal Current	In	1337,5 A	
Cosphi		1	
Efficiency	η	97,960 %	
Rotational Speed	ns	500 rpm	
Stator Parameters			
Utilization Factor	C	5,00	
Armature Loading	As	480,33 A/cm	
Inner Diameter	Di	3,51 m	
Outer Diameter	Dy	4,18 m	
Gross Iron Length	lb	0,64 m	
Net Iron Length	ln	0,56 m	
Number of Slots	Qs	198,00 slots	
Number of Cooling Ducts	nv	13,00	
Number of Turns Per Phase	Ns	66,00	
Number of Turns per Coil	tnr	1,00	
Number of Parallel Circuits	pnr	1,00	
Slots per pole and phase	q	5,50	
Relative polepitch	y	0,85	
Coil Span	Ww	14,00 slots	
Winding Factor	kw	0,93	
Sloth Height	hs	75,10 mm	
Sloth width	bu	20,88 mm	
Tooth width	bd	34,81 mm	
Slot Pitch	tu	55,69 mm	
Number of strands per bar	ndl	22,00	
Height of a Strand	hcus	2,20 mm	
Width of a Strand	bcus	7,87 mm	
Main Insulation	dij	2,13 mm	
Strand Insulation	dicu	0,10 mm	
Winding lenght	lav	3,96 m	
Cross Section of Stator Bar	Acus	373,12 mm ²	
Stator Current Density	Ss	3,58 A/mm ²	
Stator Winding Resistance	Rdc20	0,01 Ω	<i>Per Phase Resistance (20 °C)</i>
Stator Winding Resistance	Rdc75	0,02 Ω	<i>Per Phase Resistance (75 °C)</i>



C.6. OUTPUT MACHINE 2.3

Stator Wdg. Resistance Factor	Kra	1,02				
Slot Resistance Factor	Krad	1,06				
Maximum Resistance Factor	Kmax	1,19			<i>For the topmost strand</i>	
Skewing	s	0,00	slots			

Rotor Parameters

Minimum Air Gap	δ_0	11,0	mm			
Equivalent average Air Gap	δ_m	11,4	mm			
Pole Shoe width	bps	0,0	mm			
Pole Shoe Height	hps	0,0	mm			
Pole Core Width	bpc	0,0	mm			
Pole Core Height	hpc	0,0	mm			
Number of Turns per Pole	nf	0,0				
Field Current	If	0,0	A			
Field Winding Width	bcuf	0,0	mm			
Field Winding Height	hcuf	0,0	mm			
Cross Section of Field Winding	Af	0,0	mm ²			
Current Density, Field Winding	Sf	0,0	A/mm ²			
Rotor Winding Resistance	Rf20	0,0	Ω		<i>Field Wind. Resistance (20 °C)</i>	
Rotor Winding Resistance	Rf75	0,0	Ω		<i>Field Wind. Resistance (75 °C)</i>	
Relative Pole Width	α	0,70				
Number of Damperbars	NDs	0,0				
Cross Section of Damper Bar	AcuD	0,0	mm ²			
Clearance, Pole Windings	polklaring	0,0	mm			

Magnetic Parameters

Air Gap	0,852	T	0	At	<i>(peak of fundamental)</i>
Stator Core	1,212	T	0	At	
Stator Tooth	1,635	T	0	At	
Rotor Ring	1,225	T	0	At	
Pole Core/Inside PM	0,813	T	0	At	<i>(max at bottom of core)</i>
Relative Magnetization	Ef		1,141	pu	
Relative Induced Voltage	Ei		1,010	pu	
Total Required Magnetization	Θ_{mn}		0	At	
Leakage flux	FIL		1,10	%	

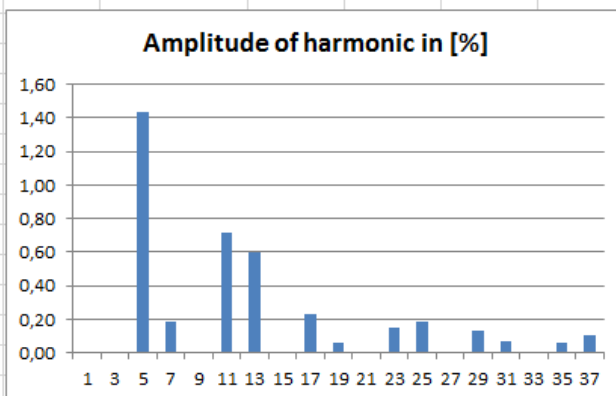
APPENDIX C. INPUT AND OUTPUT FOR THE ROTOR DESIGN

Loss Calculations				
No load:				
Iron Loss Stator Core	P _{fe}	44,7	kW	
Windage and Bearing Loss	P _{fw}	212,8	kW	
Kopper Loss Rotor (No-load)	P _{rl}	0,0	kW	
Full load:				
DC- stator loss	P _{cusdc}	86,2	kW	
AC-stator	P _{cusac}	1,7	kW	
Additional Kopper Loss Rotor	P _{rfl}	0,0	kW	
Additional loss	P _{add}	29,5	kW	
Magnetizing losses	P _{magn}	0,0	kW	
Total Losses	P _{tot}	374,9	kW	
Reactances and Time Constants				
Armature Reaction Reactance	X _{md}	0,494	pu	
	X _{mq}	0,000	pu	
Leakage Reactance	X _σ	0,102	pu	
Synchronous Reactance	X _d	0,596	pu	
	X _q	0,000	pu	
Transient Reactance	X' _d	0,000	pu	
Sub-Transient Reactance	X'' _d	0,000	pu	
	X'' _q	0,000	pu	
Transient Time Constant	T' _d	0,000	s	
Sub-Transient Time Constant	T'' _d	0,000	s	
	T'' _q	0,000	s	
Thermal Calculations				
Cooling Air Flow	q _{th}	4,8	m ³ /s	
Maximal Air Speed	v _{im}	8,9	m/s	
Mechanical Calculations				
Calculated Moment of Inertia	M	37,5	tm ²	
Weight of Machine	m	63,2	tons	
Maximum peripheral velocity	V _r	156,22	m/s	

C.6. OUTPUT MACHINE 2.3

Harmonic components in the machine

Harm.Nr.	Amplitude				
1	0,00				
3	0,00				
5	1,43				
7	0,19				
9	0,00				
11	0,72				
13	0,60				
15	0,00				
17	0,23				
19	0,06				
21	0,00				
23	0,15				
25	0,19				
27	0,00				
29	0,13				
31	0,07	Telephone Harmonic Factor	THF	0,005578 %	
33	0,00				
35	0,06				
37	0,10				



PM machine results

Remanent flux density	Br	1,14 T		
Relative permeability of PM	myr_pm	1,05		
Dimensions of PM				
Height	hpm	35,25 mm		
Surface area of each PM	Am	0,4104 m ²		
Cross-section area of each PM	Am_cross	0,0223 m ²		
Volume of each PM	V_pm	0,0142 m ³		
Totalt mass	m_pm_tot	1246,60 kg		

C.7 Input machine 2.4

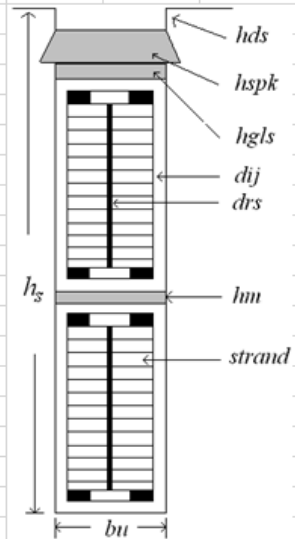
Generator specifications			
Required values:			
Apparent power	Sn	18 MVA	
Power factor	Cosphi	1	
Frequency	f	50 Hz	
Number of poles	Np	12 poles	
Runaway speed	nr	850 rpm	
Maximum temperatur rise	dTmx	60	
Moment of inertia	M	0 tm ²	
Generator maximum voltage	Vmx	15 kV	
Maximum value of synchronous reactance	xd	1,1 pu	
Maximum value of transient reactance	xd1	0,4 pu	
Minimum value of subtransient reactance	xd2	0,15 pu	
Maximum tooth flux density	Btmx	1,8 T	
Maximum pole core flux density	Bpmx	1,6 T	
Maximum yoke flux density	Bymx	1,2 T	
Specify ratio	bsdbt	0,6	
Core section length	bcs	0,04 m	
Cooling duct length	bv	0,006 m	
Filling factor (iron core)	kFe	0,95	
Current density in stator winding	Ss	3,5 A/mm ²	
Height of one strand i the statorbar	hcus	2,2 mm	
Required feild voltage	Vf	125 V	
Current density in rotor winding	Sf	3 A/mm ²	
Negative sequence voltage	Vnmx	20 %	
Skewving (in number of slots)	s	0 spor	
Outer diameter of shaft	Dri	0,3 m	
Relative pole pitch	alfa	0,7	
Remanent flux density	Br	1,14 T	
Relative permeability of PM	myr	1,05	
Optional Values:			
Do calculations for PM machine	Pmcalc	1 1=YES	0=Default
Nominal Voltage	Un	0 V	0=Default
Utilization factor	C	5,5	0=Default
Number of Slots	Qs	198	0=Default
Number of Parallel Circuits	pnr	1	0=Default
Number of Turns per Coil	tnr	1	0=Default
Coil Span	y	14 slots	0=Default

C.7. INPUT MACHINE 2.4

Inner Diameter of Stator	Di	3,51 m	0=Default
Gross Iron Length	lb	0 m	0=Default
Air Gap Flux Density	B δ	0 T	0=Default
Height of rotor yoke	hyr	0,5 m	0=Default
Cooling Air Flow	qth	0 m ³ /s	0=Default
Flywheel	GD2add	0 kg	0=Default
Minimum air gap	delta0	13 mm	0=Default
Field Winding Width	bcuf	0 m	0=Default
Specific Iron Loss, at 1 Tesla	P10	0 W/kg	0=Default
Use old iron sheets (1950-1960)	FeOld	0 1=YES	0=Default
Average Stator Coil Length	lav	0 m	0=Default
Slot Dimensions			
Slot Height	hs	0,08 m	0=Default
Slot Width	bu	0,02 m	
Number of strands in a Bar	ndl	0	
Number of Strands per Turn	ndfp	0	
Nr. of Strand on Top of each other per Turn	ndlh	0	
Total Copper Width in Slot	bcus	0 m	
Distance from Slot Wedge to Air Gap	hds	0 m	
Slot Wedge Thickness	hspk	0 m	
Slot Wedge Spacer (glidestrimmel)	hgls	0 m	
Bar Separator (mellomstrimmel)	hm	0 m	
Roebel Separator	drs	0 m	
Earth Insulation Thickness	dij	0 m	
Strand Insulation Thickness	dicu	0 m	
Winding Insulation Thickness	diw	0 m	
Pole Dimensions			
Pole Shoe Width	bps	0 m	0=Default
Pole Shoe Height	hps	0 m	0=Default
Pole Core Width	bpk	0 m	0=Default
Pole Core Height	hpk	0 m	0=Default
Total Field Winding Height	hf	0 m	0=Default
Number of turns in Field Winding	nf	0	0=Default
Height of a Field Winding	hcuf	0 m	0=Default
Number of Damper Bars	NDs	0 m	0=Default
Magnetizing Losses	Pmagn	0 kW	0=Default
Insulation between winding and pole core	bi	0 m	0=Default
Field winding insulation	bif	0 m	0=Default

C.8 Output machine 2.4

Main Data			
Apparent Power	Sn	18	MVA
System Voltage	Un	7063,5	V
Nominal Current	In	1471,3	A
Cosphi		1	
Efficiency	η	97,994	%
Rotational Speed	ns	500	rpm
Stator Parameters			
Utilization Factor	C	5,50	
Armature Loading	As	528,36	A/cm
Inner Diameter	Di	3,51	m
Outer Diameter	Dy	4,17	m
Gross Iron Length	lb	0,59	m
Net Iron Length	ln	0,52	m
Number of Slots	Qs	198,00	slots
Number of Cooling Ducts	nv	12,00	
Number of Turns Per Phase	Ns	66,00	
Number of Turns per Coil	tnr	1,00	
Number of Parallel Circuits	pnr	1,00	
Slots per pole and phase	q	5,50	
Relative polepitch	y	0,85	
Coil Span	Ww	14,00	slots
Winding Factor	kw	0,93	
Sloth Hight	hs	75,10	mm
Sloth width	bu	20,88	mm
Tooth width	bd	34,81	mm
Slot Pitch	tu	55,69	mm
Number of strands per bar	ndl	24,00	
Height of a Strand	hcus	2,20	mm
Width of a Strand	bcus	8,03	mm
Main Insulation	dij	1,96	mm
Strand Insulation	dicu	0,10	mm
Winding lenght	lav	3,86	m
Cross Section of Stator Bar	Acus	415,62	mm ²
Stator Current Density	Ss	3,54	A/mm ²
Stator Winding Resistance	Rdc20	0,01	Ω Per Phase Resistance (20 °C)
Stator Winding Resistance	Rdc75	0,01	Ω Per Phase Resistance (75 °C)



C.8. OUTPUT MACHINE 2.4

Stator Wdg. Resistance Factor	Kra	1,02			
Slot Resistance Factor	Krad	1,07			
Maximum Resistance Factor	Kmax	1,23			<i>For the topmost strand</i>
Skewing	s	0,00	slots		

Rotor Parameters

Minimum Air Gap	δ_0	13,0	mm		
Equivalent average Air Gap	δ_m	13,4	mm		
Pole Shoe width	bps	0,0	mm		
Pole Shoe Height	hps	0,0	mm		
Pole Core Width	bpc	0,0	mm		
Pole Core Height	hpc	0,0	mm		
Number of Turns per Pole	nf	0,0			
Field Current	If	0,0	A		
Field Winding Width	b _{cuf}	0,0	mm		
Field Winding Height	h _{cuf}	0,0	mm		
Cross Section of Field Winding	A _f	0,0	mm ²		
Current Density, Field Winding	S _f	0,0	A/mm ²		
Rotor Winding Resistance	R _{f20}	0,0	Ω		<i>Field Wind. Resistance (20 °C)</i>
Rotor Winding Resistance	R _{f75}	0,0	Ω		<i>Field Wind. Resistance (75 °C)</i>
Relative Pole Width	α	0,70			
Number of Damperbars	NDs	0,0			
Cross Section of Damper Bar	A _{cuD}	0,0	mm ²		
Clearance, Pole Windings	polklaring	0,0	mm		

Magnetic Parameters

Air Gap	0,835	T	0	At	<i>(peak of fundamental)</i>
Stator Core	1,214	T	0	At	
Stator Tooth	1,603	T	0	At	
Rotor Ring	0,547	T	0	At	
Pole Core/Inside PM	0,798	T	0	At	<i>(max at bottom of core)</i>
Relative Magnetization	E _f		1,148	pu	
Relative Induced Voltage	E _i		1,011	pu	
Total Required Magnetization	Θ_{mn}		0	At	
Leakage flux	FIL		1,37	%	

APPENDIX C. INPUT AND OUTPUT FOR THE ROTOR DESIGN

Loss Calculations				
No load:				
Iron Loss Stator Core	P _{fe}	40,5	kW	
Windage and Bearing Loss	P _{fw}	205,0	kW	
Kopper Loss Rotor (No-load)	P _{rl}	0,0	kW	
Full load:				
DC- stator loss	P _{cusdc}	91,5	kW	
AC-stator	P _{cusac}	2,1	kW	
Additional Kopper Loss Rotor	P _{rfl}	0,0	kW	
Additional loss	P _{add}	29,3	kW	
Magnetizing losses	P _{magn}	0,0	kW	
Total Losses	P _{tot}	368,4	kW	
Reactances and Time Constants				
Armature Reaction Reactance	X _{md}	0,498	pu	
	X _{mq}	0,000	pu	
Leakage Reactance	X _σ	0,113	pu	
	X _d	0,610	pu	
Synchronous Reactance	X _q	0,000	pu	
	X' _d	0,000	pu	
Transient Reactance	X'' _d	0,000	pu	
	X'' _q	0,000	pu	
Transient Time Constant	T' _d	0,000	s	
Sub-Transient Time Constant	T'' _d	0,000	s	
	T'' _q	0,000	s	
Thermal Calculations				
Cooling Air Flow	q _{th}	4,8	m ³ /s	
Maximal Air Speed	v _{im}	9,7	m/s	
Mechanical Calculations				
Calculated Moment of Inertia	M	56,2	tm ²	
Weight of Machine	m	82,9	tons	
Maximum peripheral velocity	V _r	156,22	m/s	

Harmonic components in the machine

Harm.Nr.	Amplitude
1	0,00
3	0,00
5	1,43
7	0,19
9	0,00
11	0,72
13	0,60
15	0,00
17	0,23
19	0,06
21	0,00
23	0,15
25	0,19
27	0,00
29	0,13
31	0,07
33	0,00
35	0,06
37	0,10

Amplitude of harmonic in [%]

Harmonic Order	Amplitude [%]
1	0.00
3	0.00
5	1.43
7	0.19
9	0.00
11	0.72
13	0.60
15	0.00
17	0.23
19	0.06
21	0.00
23	0.15
25	0.19
27	0.00
29	0.13
31	0.07
33	0.00
35	0.06
37	0.10

Telephone Harmonic Factor	THF	0,005578 %
---------------------------	-----	------------

PM machine results

Remanent flux density	Br	1,14 T
Relative permeability of PM	myr_pm	1,05
Dimensions of PM		
Height	hpm	38,62 mm
Surface area of each PM	Am	0,3808 m ²
Cross-section area of each PM	Am_cross	0,0244 m ²
Volume of each PM	V_pm	0,0144 m ³
Totalt mass	m_pm_tot	1264,58 kg

Appendix D

Attached files

The following files are regarded as attachment to this thesis:

- **GenProgv2.m** - The Matlab script performing the computation of the synchronous machine. This script is capable to do calculations for both field winding as well as PM synchronous machines.
- **Int.m** - Matlab function to make calculations for magnetic voltage drop. *GenProgv2* is calling this function.
- **Input.xls** - Excel sheet to define values of input parameters used in the computation. *GenProgv2* is reading from this file.
- **Output.xls** - Excel sheet to present output parameters from the computation. *GenProgv2* is writing to this file.
- **sporfil.xls** - Excel sheet to present different possible number of stator slots. *GenProgv2* is writing to this file.